14-3-3γ binds regulator of G protein signaling 14 (RGS14) at distinct sites to inhibit the RGS14:Gα_i–AlF_4^- signaling complex and RGS14 nuclear localization

Received for publication, March 9, 2018, and in revised form, July 23, 2018 Published, Papers in Press, August 9, 2018, DOI 10.1074/jbc.RA118.002816

Kyle J. Gerber, Katherine E. Squires, and John R. Hepler[1]

From the Department of Pharmacology, Emory University School of Medicine, Atlanta, Georgia 30322

Edited by Henrik G. Dohlman

Regulator of G protein signaling 14 (RGS14) is a multifunctional brain scaffolding protein that integrates G protein and Ras/ERK signaling pathways. It is also a nucleocytoplasmic shuttling protein. RGS14 binds active G$\alpha_{i/o}$ via its RGS domain, Raf and active H-Ras–GTP via its R1 Ras-binding domain (RBD), and inactive G$\alpha_{i1/3}$ via its G protein regulatory (GPR) domain. RGS14 suppresses long-term potentiation (LTP) in the CA2 region of the hippocampus, thereby regulating hippocampally based learning and memory. The 14-3-3 family of proteins is necessary for hippocampal LTP and associative learning and memory. Here, we show direct interaction between RGS14 and 14-3-3γ at two distinct sties, one phosphorylation-independent and the other phosphorylation-dependent at Ser-218 that is markedly potentiated by signaling downstream of active H-Ras. Using bioluminescence resonance energy transfer (BRET), we show that the pSer-218 – dependent RGS14/14-3-3γ interaction inhibits active Gα_{i1}–AlF_4^- binding to the RGS domain of RGS14 but has no effect on active H-Ras and inactive Gα_{i1}–GDP binding to RGS14. By contrast, the phosphorylation-independent binding of 14-3-3 has no effect on RGS14/Gα_i interactions but, instead, inhibits (directly or indirectly) RGS14 nuclear import and nucleocytoplasmic shuttling. Together, our findings describe a novel mechanism of negative regulation of RGS14 functions, specifically interactions with active Gα_i and nuclear import, while leaving the function of other RGS14 domains intact. Ongoing studies will further elucidate the physiological function of this interaction between RGS14 and 14-3-3γ, providing insight into the functions of both RGS14 and 14-3-3 in their roles in modulating synaptic plasticity in the hippocampus.

The regulator of G protein signaling (RGS)[2] and RGS-like family of proteins (nearly 40 members) is characterized by their GTPase-activating protein activity on G protein α (Gα) subunits (1, 2). One RGS protein family member, RGS14, is an unusual brain scaffolding protein that integrates G protein and mitogen-activated protein kinase signaling pathways to regulate synaptic plasticity relating to hippocampally based learning and memory (3). RGS14 integrates signaling through multiple GTPases by binding active G$\alpha_{i/o}$ subunits (4), inactive Gα_{i1} and Gα_{i3} (5), and small GTPases, including active H-Ras (6, 7) and Rap2 (8). Besides binding G$\alpha_{i/o}$ at its RGS domain, RGS14 also interacts with GDP-bound G$\alpha_{i1/3}$ subunits at its G protein regulatory (GPR) motif (4, 5, 9, 10). Although RGS14 was originally discovered as a Rap-binding protein via its R1 Raf-like Ras/Rap-binding domain, studies suggest that RGS14 likely interacts preferentially with active H-Ras in cells (6, 7). RGS14 also interacts with both G protein– couple receptors and the nonreceptor guanine nucleotide exchange factor Ric-8A in a G protein–dependent manner (6, 10, 11). Whereas RGS14 interacts with multiple signaling proteins at the plasma membrane, we and others have shown that RGS14 is also a nucleocytoplasmic shuttling protein (5, 12–14), suggesting it serves as yet undefined roles in the nucleus.

Although RGS14 binds to a variety of signaling GTPases, other regulatory protein-binding partners have not been identified. Members of the 14-3-3 family of proteins are ubiquitous regulatory proteins abundant in brain (15). They consist of seven distinct isoforms in mammals, although differences in their function are largely unclear, with all 14-3-3 isoforms often referred to generally as 14-3-3 proteins (16–19). These proteins exist as dimers (20, 21) with each monomer capable of interacting with a distinct 14-3-3– binding site (22, 23), typically centered at a phosphorylated serine or threonine (22, 24, 25), although there are exceptions (26–31). In some cases, 14-3-3 can bind to poorly defined protein sequences in a phosphorylation-independent manner (26–31). Upon binding, 14-3-3 proteins exert multiple effects on their substrates, including changes in conformation, masking of binding sites for other proteins (26), and changes in subcellular localization (17, 21, 26,

This work was supported by National Institutes of Health Grants 5R01NS037112 and 1R21NS087488 (to J. R. H.), Grant F31NS098648 (to K. J. G.), and Training Grant T32 GM008602 (to K. J. G. and K. E. S.). The authors declare that they have no conflicts of interest with the contents of this article. The content is solely the responsibility of the authors and does not necessarily represent the official views of the National Institutes of Health.

This article contains Figs. S1–S4.

[1] To whom correspondence should be addressed: Dept. of Pharmacology, Emory University School of Medicine, 1510 Clifton Rd., Rollins Research Center, Suite G205, Atlanta, GA 30322. Tel.: 404-727-3641; E-mail: jhepler@emory.edu.

[2] The abbreviations used are: RGS, regulator of G protein signaling; BRET, bioluminescence resonance energy transfer; GPR, G protein regulatory; LMB, leptomycin B; LTP, long-term potentiation; RBD, Ras-binding domain; ERK, extracellular signal-regulated kinase; HEK, human embryonic kidney; MEK, mitogen-activated protein kinase/extracellular signal-regulated kinase kinase; CaMKII, Ca^{2+}/calmodulin-dependent protein kinase II; PI3K, phosphatidylinositol 3-kinase; EGF, epidermal growth factor; Luc, luciferase; YFP, yellow fluorescent protein; MBP, maltose-binding protein; TEV, tobacco etch virus; HRP, horseradish peroxidase; TBS, Tris-buffered saline; PEI, polyethyleneimine; HBSS, Hanks' balanced salt solution; IACUC, Institutional Animal Care and Use Committee.

32–34). 14-3-3 has been shown to interact with multiple RGS proteins, including RGS4, RGS5, RGS16 (26), RGS3 (35–38), and RGS7 (35, 39). In many of these cases, 14-3-3 association with phosphorylated residues within the RGS domain results in inhibition of GTPase-activating protein activity (26, 35, 37, 38), providing a mechanism through which posttranslational modification can negatively regulate the impact of an RGS protein on G protein signaling. Additionally, 14-3-3 proteins are reported to affect the subcellular localization of RGS4, sequestering it in the cytoplasm and preventing its recruitment to the plasma membrane by active Gα (26).

Although RGS14 interaction with Gα_i–GTP has been shown to be enhanced by phosphorylation (40), no clear mechanism for the negative regulation of RGS14 interactions with Gα_i has been identified. Here, we report that native RGS14 forms a stable complex with 14-3-3 in the hippocampus where RGS14 has been shown to negatively regulate synaptic plasticity and, consequently, learning and memory (3). 14-3-3 binds RGS14 at two distinct sites, one phosphorylation-dependent and the other phosphorylation-independent. In HEK 293 cells, we found that RGS14 binds 14-3-3γ selectively and that this interaction is markedly potentiated by downstream active H-Ras signaling. This interaction is phosphorylation-dependent, and complex formation between RGS14 and 14-3-3 occurs directly, independently of any other interacting partners. 14-3-3 binding is centered at phosphorylated serine 218, and binding at that site inhibits active Gα_i binding at the RGS domain of RGS14 without affecting inactive Gα_i interaction with the GPR motif or active H-Ras binding at the R1 domain. In hippocampal neurons, the cell type in which RGS14 is natively expressed in the brain (13, 41), we report that 14-3-3 also binds at a second site in a phosphorylation-independent manner. This 14-3-3 binding is distinct from that at phosphoserine 218. RGS14 is a nucleocytoplasmic shuttling protein (5, 12, 14), and 14-3-3 prevents RGS14 nuclear import in hippocampal neurons independently of binding to phospho-Ser-218.

Overall, our findings provide clear evidence for distinct phosphorylation-dependent and phosphorylation-independent binding sites for 14-3-3 on RGS14. Binding of 14-3-3 at these sites negatively regulates RGS14 interaction with active Gα_i at the RGS domain and nuclear import, respectively, demonstrating two distinct mechanisms through which 14-3-3 modulates RGS14 function and subcellular localization in hippocampal neurons.

Results

Previous work reported that 14-3-3 regulates the functions of several RGS proteins (26, 35–39). To explore the possibility that 14-3-3 might bind to and regulate the function of RGS14, we immunoprecipitated native RGS14 out of mouse brain and subsequently probed for interactions with 14-3-3 proteins via immunoblotting (Fig. 1). Because RGS14 is highly and selectively expressed in the CA2 area of the hippocampus (41), we used isolated hippocampi as a tissue source for these studies. 14-3-3γ was highly enriched in samples in which RGS14 was specifically immunoprecipitated as opposed to the beads-only condition where RGS14 was not enriched (Fig. 1). In combination, these data show that endogenously expressed 14-3-3 specifically interacts with native RGS14 from the CA2 region of the mouse hippocampus.

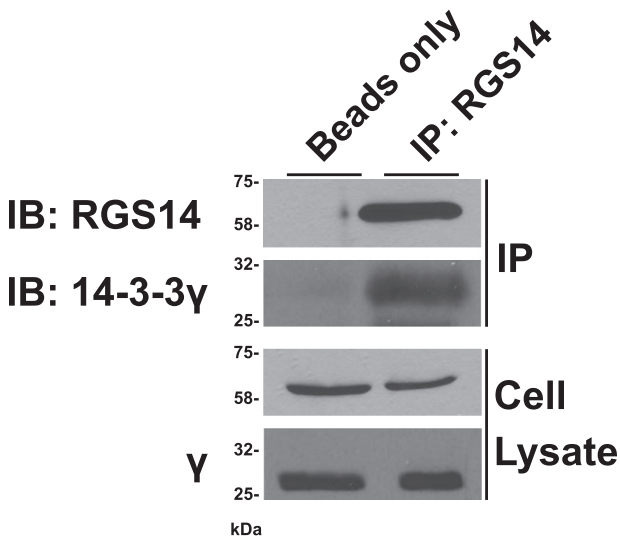

Figure 1. Native RGS14 interacts with endogenous 14-3-3γ in mouse hippocampus. Both hippocampi from an adult mouse were isolated and homogenized with lysis buffer to generate cell lysate. Half of the lysate was incubated with anti-RGS14 antibody (*IP: RGS14*) and protein G-Sepharose beads, and the other half was incubated with beads alone (*Beads only*). Beads were then washed, and recovered proteins were resolved using SDS-PAGE before being subjected to immunoblotting (*IB*). The cell lysate immunoblots represent 2% of the whole-cell lysates used for the immunoprecipitation (*IP*).

To better understand the subcellular signaling events that affect and control the interaction between RGS14 and 14-3-3, we transitioned to the more manipulation-friendly system of transient transfection in HEK 293 cells. Following FLAG immunoprecipitation from HEK 293 cells expressing FLAG-tagged RGS14 (FLAG–RGS14) and 14-3-3γ, we saw little or no interaction between RGS14 and 14-3-3 (Fig. 2*A*) when compared with a baseline condition in which the immunoprecipitation was performed in the absence of RGS14 and the presence of 14-3-3. However, when RGS14's binding partner at the R1 domain, active H-Ras(G12V) (6, 7), was expressed along with RGS14 and 14-3-3γ, we observed a clear interaction. The specificity of this interaction was further validated by the inclusion of a condition in which 14-3-3γ(K50E), which contains a mutation in the amphipathic helix of 14-3-3 that significantly decreases affinity for known 14-3-3 substrates (42, 43), was expressed. As expected, 14-3-3γ(K50E) showed decreased binding when compared with the wildtype (WT) protein (Fig. 2*A*), indicating that induction of 14-3-3 association with RGS14 by active H-Ras is specific.

Because active H-Ras has been reported to interact directly with RGS14 (6, 7, 44, 45), it was unclear whether downstream H-Ras signaling or direct H-Ras binding to RGS14 was responsible for its induction of a 14-3-3γ:RGS14 complex. To parse out the role of active H-Ras in relation to 14-3-3γ and RGS14, we used a mutation, RGS14(R333L), that has been shown to greatly reduce binding of H-Ras at the R1 domain (6, 45). Using RGS14(R333L), any observed enhancement of the RGS14/14-3-3γ interaction by active H-Ras can be attributed only to downstream signaling of H-Ras and not direct interaction with RGS14. We saw no difference in 14-3-3γ binding to RGS14 or RGS14(R333L) in the presence of active H-Ras (Fig. 2*B*), indi-

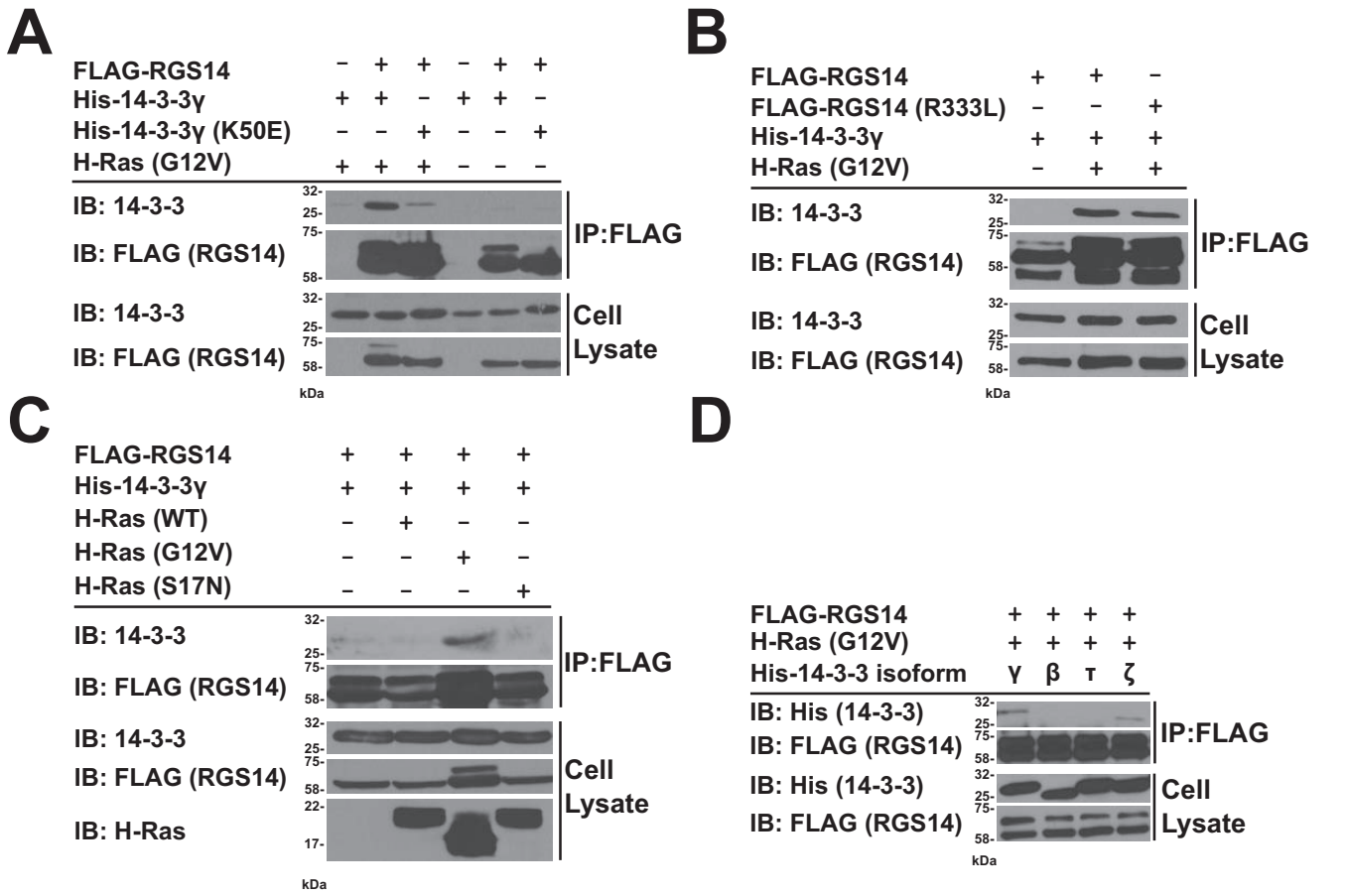

Figure 2. RGS14-specific association with 14-3-3γ is promoted by signaling events downstream of active H-Ras. *A*, active H-Ras enhances RGS14 association with 14-3-3γ. 10-cm dishes of HEK 293 cells were transfected with 1.5 μg of FLAG–RGS14, 3 μg of His-tagged 14-3-3γ (*His-14-3-3γ*), 3 μg of a binding-incompetent mutant of 14-3-3γ (14-3-3γ(K50E)), and/or 1.5 μg of constitutively active H-Ras (H-Ras(G12V)) as indicated. Whole-cell lysates were subjected to FLAG immunoprecipitation (*IP: FLAG*), and recovered proteins were subjected to SDS-PAGE followed by immunoblotting (*IB*). *B*, active H-Ras does not influence 14-3-3 binding through direct interaction with RGS14. HEK 293 cells were transfected with 1.5 μg of FLAG–RGS14, 3 μg of His-tagged 14-3-3γ, 1.5 μg of active H-Ras, and/or a 1.5 μg of a point mutant of RGS14 that demonstrates greatly decreased binding to Ras (FLAG–RGS14(R333L)). Samples were collected and subjected to FLAG immunoprecipitation and SDS-PAGE, and analyzed via immunoblotting. *C*, H-Ras must be active to potentiate RGS14/14-3-3 interaction. 1.5 μg of FLAG–RGS14 and 3 μg of His-tagged 14-3-3γ were transfected into HEK 293 cells along with either 1.5 μg of empty vector, 1.5 μg of WT, 1.5 μg of constitutively active (G12V), or 1.5 μg of dominant-negative (S17N) H-Ras. RGS14 and associated proteins were isolated via FLAG immunoprecipitation and subjected to SDS-PAGE before being analyzed using immunoblotting. *D*, RGS14 selectively interacts with the γ isoform of 14-3-3. HEK 293 cells were transfected overnight with FLAG–RGS14, H-Ras(G12V), and His-tagged 14-3-3γ, -β, -τ, or -ζ. Samples were then lysed and subjected to FLAG immunoprecipitation before being subjected to SDS-PAGE and analyzed for 14-3-3 interactions with RGS14 by immunoblotting for the hexahistidine tag on the 14-3-3 isoforms. The cell lysate immunoblots represent 2% of the whole-cell lysates used for the immunoprecipitation. These findings are representative of three independent experiments.

cating that H-Ras induces RGS14 association with 14-3-3γ through a downstream signaling mechanism.

To further confirm that downstream signaling by active H-Ras is necessary to promote 14-3-3γ interaction with RGS14 in HEK 293 cells, we immunoprecipitated FLAG–RGS14 and probed for an interaction with 14-3-3γ in the presence of active H-Ras(G12V), WT H-Ras, and the dominant-negative mutant H-Ras(S17N). As expected, only H-Ras(G12V) greatly enhanced 14-3-3 binding to RGS14 (Fig. 2*C*), indicating that downstream signaling through active H-Ras is necessary for the potentiation of the interaction between RGS14 and 14-3-3.

To test for possible specific interactions between RGS14 and distinct 14-3-3 isoforms, we performed a screen of multiple 14-3-3 isoforms (β, γ, τ, and ζ) in the presence of H-Ras(G12V). We blotted for the hexahistidine tag on each of the 14-3-3 isoforms following immunoprecipitation of FLAG–RGS14 so that all of the isoforms could be compared equally. Besides 14-3-3γ, 14-3-3ζ also appeared to interact with RGS14 with 14-3-3γ appearing to interact most strongly (Fig. 2*D*). Therefore, our subsequent studies focused on the specific interaction between RGS14 and 14-3-3γ.

14-3-3 proteins typically bind substrates at specific motifs centered at a phosphorylated serine or threonine (24, 25). However, 14-3-3 proteins are also capable of binding target proteins at nonphosphorylated residues (26–31). To determine whether the H-Ras–potentiated 14-3-3γ interaction with RGS14 was phosphorylation-dependent, we overexpressed FLAG–RGS14 and 14-3-3γ and immunoprecipitated RGS14 from HEK 293 cells in the presence or absence of constitutively active H-Ras(G12V). Samples were either collected in the presence of a phosphatase inhibitor mixture to preserve phosphorylation sites or treated with λ-phosphatase to dephosphorylate any phosphorylated residues on RGS14. Although little interaction between RGS14 and 14-3-3γ was seen in the absence of

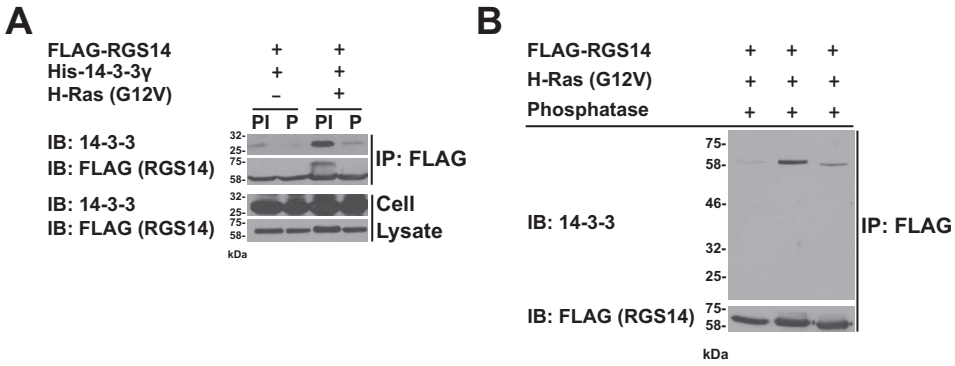

Figure 3. 14-3-3γ directly binds RGS14 in a phosphorylation-dependent manner. *A*, 14-3-3 binds RGS14 in a phosphorylation-dependent manner. HEK 293 cells were transfected with 1.5 μg of FLAG–RGS14 and 3 μg of His-tagged 14-3-3γ either in the presence or absence of 1.5 μg of overexpressed H-Ras(G12V). Samples were either lysed in buffer containing a phosphatase inhibitor mixture (*PI*) or treated with λ-phosphatase following lysis (*P*). All samples were then incubated with anti-FLAG M2 affinity gel to pull down any proteins associated with FLAG–RGS14. The gel was washed, and samples were denatured in Laemmli buffer before being subjected to SDS-PAGE and immunoblotting (*IB*). *B*, 14-3-3 interacts directly with RGS14 in far-Western blotting. HEK 293 cells were transfected with FLAG–RGS14 either in the presence or absence of overexpressed H-Ras(G12V). All samples were then incubated with anti-FLAG M2 affinity gel to separate RGS14 from the whole-cell lysate. Samples were then either denatured in Laemmli buffer or treated with λ-phosphatase and then subjected to SDS-PAGE and transferred to a nitrocellulose membrane, which was incubated with pure His-tagged 14-3-3γ overnight and probed for interactions between RGS14 and 14-3-3 via immunoblotting for 14-3-3. The cell lysate immunoblots represent 2% of the whole-cell lysates used for the immunoprecipitation (*IP*). These findings are representative of three independent experiments.

active H-Ras, the sample collected in the presence of both the phosphatase inhibitor mixture and H-Ras(G12V) showed a robust interaction between RGS14 and 14-3-3γ. Notably, the sample collected in the absence of phosphatase inhibitor mixture and treated with λ-phosphatase showed a greatly reduced interaction compared with the positive control (Fig. 3*A*), indicating that 14-3-3γ interacts with RGS14 through a phosphorylated serine or threonine.

One major caveat of using coimmunoprecipitation from whole cells as a technique to examine protein/protein interactions is the inability to determine whether an interaction between two proteins is direct or indirect. In the case of RGS14, it was imperative to determine whether 14-3-3γ binding to RGS14 was direct because RGS14 is reported to interact with Raf in an active H-Ras–dependent manner (45), and Raf is a well known binding partner of 14-3-3 (20, 24, 31, 42, 46–49). Therefore, we used a far-Western blotting overlay experiment to determine whether 14-3-3γ is capable of binding to RGS14 directly under the same conditions in which it interacts with RGS14 using coimmunoprecipitation (Fig. 3*B*). FLAG–RGS14 expressed in HEK 293 cells in the presence or absence of H-Ras(G12V) was immunoprecipitated to enrich the RGS14 in each sample. The samples were denatured, run on an SDS-polyacrylamide gel, and transferred to a nitrocellulose membrane, which was incubated overnight with pure 14-3-3γ protein. 14-3-3γ binding to RGS14 was detected by immunoblotting of the nitrocellulose membrane. We found that purified 14-3-3γ interacts directly with the denatured RGS14 bands in the membrane at the correct size, 61 kDa (14-3-3γ is ~28 kDa) in the same manner as predicted by previous coimmunoprecipitation experiments. Active H-Ras greatly increased 14-3-3γ binding to RGS14, whereas treatment of an identical sample with λ-phosphatase greatly decreased this interaction (Fig. 3*B*). This indicates that 14-3-3γ interacts directly with phosphorylated RGS14 with no other protein necessary as part of a complex to mediate the interaction.

Knowing that 14-3-3γ interacts directly with RGS14 at a typical 14-3-3–binding motif centered at a phosphorylated serine or threonine, we created truncations of RGS14 to map the location of the 14-3-3γ–binding site (Fig. 4*A*). All truncated proteins were created with an N-terminal FLAG tag so they could be immunoprecipitated equally and their expression could be directly compared. Full-length FLAG–RGS14 and the four truncations were expressed in HEK 293 cells with 14-3-3γ and active H-Ras and subjected to FLAG immunoprecipitation. Notably, only RGS14 constructs that contained the linker region between the RGS domain and the tandem RBDs (constructs *1*, *3*, and *4*) coimmunoprecipitated with 14-3-3γ (Fig. 4*B*), indicating that 14-3-3γ binds a site within that linker region including RGS14 residues 186–301 (Fig. 4).

Having mapped the possible 14-3-3γ–binding site to the linker region between the RGS and R1 domains, we submitted the RGS14 amino acid sequence to Scansite3 to identify possible 14-3-3γ–binding motifs (50). At low stringency, Scansite3 predicted seven possible 14-3-3–binding motifs throughout RGS14 with three of those sites included within residues 205–301, the region determined to contain the 14-3-3γ–binding site by the truncations. Although mutation of serines 258 and 286 to phospho-null alanines had no effect on 14-3-3γ association with RGS14 (Fig. S1), mutation of serine 218 to alanine (RGS14(S218A)) greatly decreased H-Ras–potentiated binding of 14-3-3 to RGS14 (Fig. 5*B*). Furthermore, serine 218 and the surrounding region are completely conserved in human, rat, and mouse RGS14 (Fig. 5*A*), and serine 218 has been shown to be phosphorylated in multiple MS experiments (51) with peptides unique to RGS14 being found to contain phospho-Ser-218 of RGS14 from rat (52, 53), mouse (54), and human (55) cells. Taken together, these findings show that RGS14 contains a conserved 14-3-3γ–binding motif centered at serine 218.

Knowing the specific site at which 14-3-3 binds RGS14, we next attempted to determine the kinase that phosphorylates serine 218 of RGS14 to better understand the role that 14-3-3 interaction with RGS14 plays in relation to both RGS14 and 14-3-3 signaling. We focused on MEK, Akt, and CaMKII as possible kinases that could phosphorylate serine 218 because all of these kinases are downstream of active H-Ras signaling and

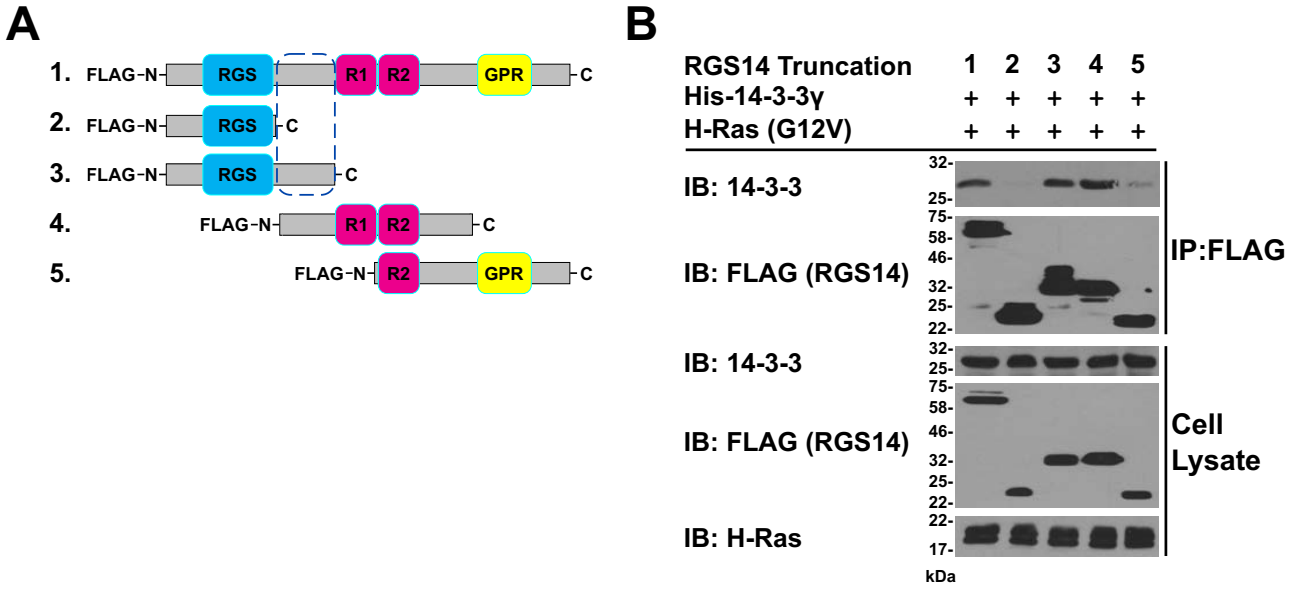

Figure 4. 14-3-3γ binds the linker region between the RGS and tandem R1/R2 domains of RGS14. *A*, truncation mutants of RGS14 with FLAG tags on the N-terminal end of the protein were made to determine the 14-3-3– binding site. Mutant *1* is full-length rat RGS14 composed of 544 amino acids discounting the FLAG tag. Mutant *2* contains the RGS domain and encodes for amino acids 1–202 of RGS14. Mutant *3* contains the RGS domains as well as the linker region between the RGS domain and R1, ending at residue 300. Mutant *4* contains both Raf-like Ras-binding domains (R1 and R2) and residues 205–490. Mutant *5* consists of amino acids 371–544 and contains both the R2 and GPR domains. HEK 293 cells were transfected with these constructs (1.5 μg), 3 μg of His-tagged 14-3-3γ, and 1.5 μg of H-Ras(G12V). *B*, samples were collected and incubated with anti-FLAG M2 affinity gel to pull down the FLAG–RGS14 and associated proteins. These samples were then subjected to SDS-PAGE and immunoblotting (*IB*) with the indicated antibodies. The cell lysate immunoblots represent 2% of the whole-cell lysates used for the immunoprecipitation (*IP*). These findings are representative of three independent experiments.

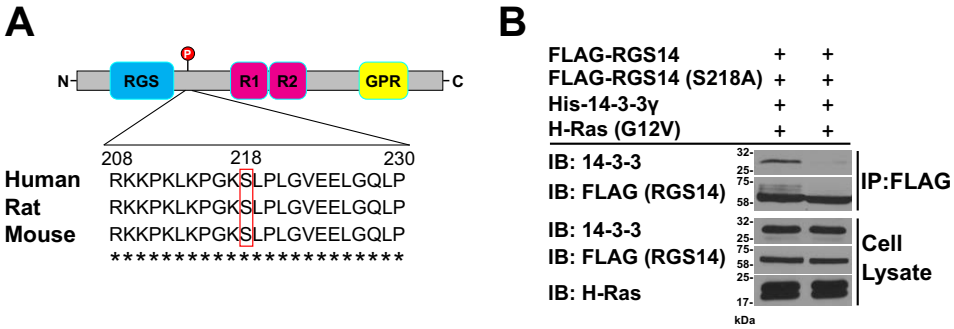

Figure 5. 14-3-3γ binds RGS14 at serine 218. *A*, alignment of the human, rat, and mouse RGS14 amino acid sequences shows complete conservation of serine 218 and surrounding amino acids. *B*, mutation of serine 218 of RGS14 to a phospho-null alanine decreases RGS14's association with 14-3-3. 1.5 μg of WT RGS14 or 1.5 μg of RGS14(S218A) were expressed in HEK 293 cells in the presence of 3 μg of His-tagged 14-3-3γ and 1.5 μg of active H-Ras. Lysates were collected and subjected to FLAG immunoprecipitation before being analyzed by SDS-PAGE followed by immunoblotting (*IB*). The cell lysate immunoblots represent 2% of the whole-cell lysates used for the immunoprecipitation (*IP*). These findings are representative of three independent experiments.

because Akt and CaMKII are both predicted to phosphorylate serine 218 by Scansite3 (50) under the minimum stringency. Following treatment of HEK 293 cells expressing FLAG–RGS14, 14-3-3γ, and H-Ras(G12V) with selective inhibitors of either MEK (U0126), PI3K (LY294002), or CaMKII (KN-93) for 2 h, cells were collected, subjected to FLAG immunoprecipitation, and probed for RGS14/14-3-3 interactions. However, none of the kinase inhibitors had any effect (Fig. S2*A*), indicating that ERK, Akt, and CaMKII are not responsible for the phosphorylation of serine 218 of RGS14.

We next tested whether acute activation of endogenous H-Ras is sufficient to promote 14-3-3γ binding to RGS14 or whether long-term activation is necessary. To activate endogenous Ras acutely, HEK 293 cells expressing FLAG–RGS14 and 14-3-3γ were treated with EGF for 0, 10, 60, or 120 min. EGF treatment did not markedly enhance RGS14 pulldown of 14-3-3γ at the earlier time points, but increased interaction was evident at the 2-h time point, indicating that prolonged H-Ras signaling is necessary (Fig. S2*B*). This suggests that changes at a protein translation level are likely necessary to enhance the RGS14/14-3-3 interaction in HEK cells. These findings indicate that the kinase responsible for phosphorylating serine 218 of RGS14 is unlikely to be directly downstream of active H-Ras, making the kinase responsible immensely difficult to predict and identify. Therefore, in subsequent efforts to identify a function for 14-3-3γ interaction with RGS14, we focused on the functional consequences of 14-3-3γ binding to RGS14 rather than the specific phosphorylation site and responsible kinase.

14-3-3 has been shown to interact with multiple RGS proteins (26, 35, 37, 38), competing with Gα for binding at the RGS domain and consequently inhibiting GTPase activity (26, 35). Interestingly, even 14-3-3 binding near but outside of the RGS

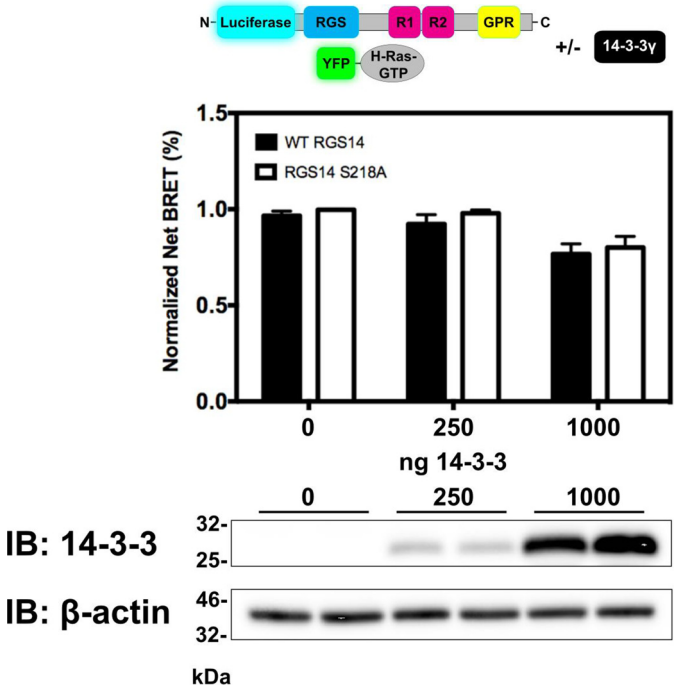

Figure 6. RGS14/14-3-3γ interaction does not affect H-Ras binding at the R1 domain. 6-well plates of HEK 293 cells were transfected with 500 ng of H-Ras(G12V)–Venus and 10 ng of WT or S218A RGS14–luciferase with increasing amounts of 14-3-3γ (0, 250, or 1000 ng of plasmid). BRET ratios for the interaction between H-Ras(G12V) and RGS14–Luc or RGS14(S218A)–Luc were recorded, and the net BRET signal was calculated by subtracting the BRET signal from RGS14–Luc or RGS14(S218A) alone, respectively. Net BRET was normalized with maximum net BRET (0.0978) given a value of 1 and plotted against the acceptor (Venus)/donor (luciferase) ratio. Data shown are the pooled mean ± S.E. (*error bars*) of three separate experiments, each with triplicate determinations. Representative immunoblots showing expression levels of 14-3-3γ are shown below along with a β-actin loading control. *IB*, immunoblotting.

domain of RGS3 has been shown to block G protein binding (36). Because of the relatively close proximity of the 14-3-3γ-binding site on RGS14 to the RGS domain (33 amino acids away), we examined the effect of 14-3-3γ binding to RGS14 on its interactions with active H-Ras(G12V) at the R1 domain as well as active $G\alpha_{i1}$ binding at the RGS domain. For this, we examined protein/protein interactions in live cells using bioluminescence resonance energy transfer (BRET).

To determine whether 14-3-3γ binding to RGS14 affects H-Ras(G12V) interaction with RGS14 at the R1 domain, we used BRET to measure the interaction of H-Ras(G12V)–Venus with RGS14–luciferase (Luc) in the presence of increasing expression of 14-3-3γ. As a control for specific 14-3-3γ binding to RGS14, we compared active H-Ras binding to WT RGS14 with H-Ras interaction with RGS14(S218A). We saw no difference in H-Ras(G12V)–Venus interaction with RGS14–Luc or RGS14(S218A)–Luc at any level of 14-3-3γ expression (Fig. 6), indicating that 14-3-3γ does not affect active H-Ras(G12V) binding to RGS14.

We next sought to determine whether 14-3-3 affects active $G\alpha_{i1}$ binding at the RGS domain of RGS14. Following incubation of HEK 293 cells expressing H-Ras(G12V), Luc–RGS14, and $G\alpha_{i1}$–YFP with AlF_4^-, a nonspecific activator of heterotrimeric Gα subunits, we measured binding of $G\alpha_{i1}$ at the RGS domain of RGS14. With the addition of overexpressed 14-3-3γ, the maximum measured interaction between $G\alpha_{i1}$–AlF_4^- and RGS14 was decreased by ~50% (Fig. 7*A*), indicating that binding of 14-3-3γ to RGS14 inhibits G protein binding at the RGS domain. We also performed this experiment with Luc–RGS14(S218A) to confirm that 14-3-3γ binding centered at serine 218, as opposed to a possible off-target effect, was responsible for inhibition of active $G\alpha_{i1}$ binding at the RGS domain. Using this Luc–RGS14(S218A) point mutant, we saw no effect on maximal G protein binding when 14-3-3γ was overexpressed (Fig. 7*B*). Furthermore, to examine whether 14-3-3γ inhibition of $G\alpha_{i1}$ interaction with RGS14 is specific to the RGS domain, we performed the same experiment in the absence of AlF_4^- with RGS14–Luc to measure any contributions that 14-3-3γ binding to RGS14 might have to $G\alpha_{i1}$ binding to the GPR motif at the C-terminal end of the protein. In this case, expression of 14-3-3γ had no effect (Fig. 7*C*), indicating that 14-3-3γ binding to RGS14 only decreases active $G\alpha_{i1}$ interaction with the RGS domain.

After demonstrating that 14-3-3 specifically affects $G\alpha_{i1}$ binding to the RGS domain of RGS14, we next sought to examine the effect of 14-3-3 on RGS14 subcellular localization because 14-3-3 proteins have been shown to often affect the distribution of binding partners within the cell (17, 21, 26). We and others have previously shown that although RGS14 is predominantly cytosolic it is nonetheless a nucleocytoplasmic shuttling protein (5, 12, 13) as demonstrated by the fact that treatment of HEK cells with leptomycin B (LMB), which inhibits its nuclear export, leads to a buildup of RGS14 in the nucleus as it is constantly being imported but unable to be shuttled out of the nucleus (5, 12). Here, we show that YFP–RGS14 shuttles in and out of the nucleus in primary hippocampal neurons, the cell type in which RGS14 is natively expressed in the adult brain (41) (Fig. 8). Notably, coexpression of 14-3-3γ prevented RGS14 translocation into the nucleus over the course of a 2-h treatment with LMB. Furthermore, coexpression of the binding-null mutant 14-3-3γ(K50E) with RGS14 still allowed RGS14 to be transported into the nucleus (Fig. 8), indicating that 14-3-3γ is binding specifically to substrates in the cell, presumably RGS14, to block RGS14 nuclear localization.

Next, we tested RGS14(S218A) to determine whether 14-3-3's interaction with RGS14 at that specific site contributed to its effect on RGS14's nuclear localization. Quite unexpectedly, RGS14(S218A) behaved identically to WT RGS14 in the presence of 14-3-3γ following treatment with LMB. 14-3-3γ was still able to prevent transport of RGS14(S218) into the nucleus (Fig. 9), suggesting the possibility of a second 14-3-3γ– binding site on RGS14 with its own distinct function.

To explore this idea of a second 14-3-3– binding site and in an effort to make sense of 14-3-3's effect on RGS14 nuclear localization, we reexamined previous data (Fig. 3*B*), noticing faint bands in the control conditions in the far-Western blot. These findings were consistent with direct 14-3-3 binding to RGS14, thus providing evidence of a potential second, phosphorylation-independent binding site on RGS14 for 14-3-3γ. To test this idea, we again performed a far-Western experiment (Fig. 10), this time comparing 14-3-3 binding to RGS14 immunoprecipitated from HEK cells (not treated with constitutively active H-Ras and therefore not strongly phosphorylated at ser-

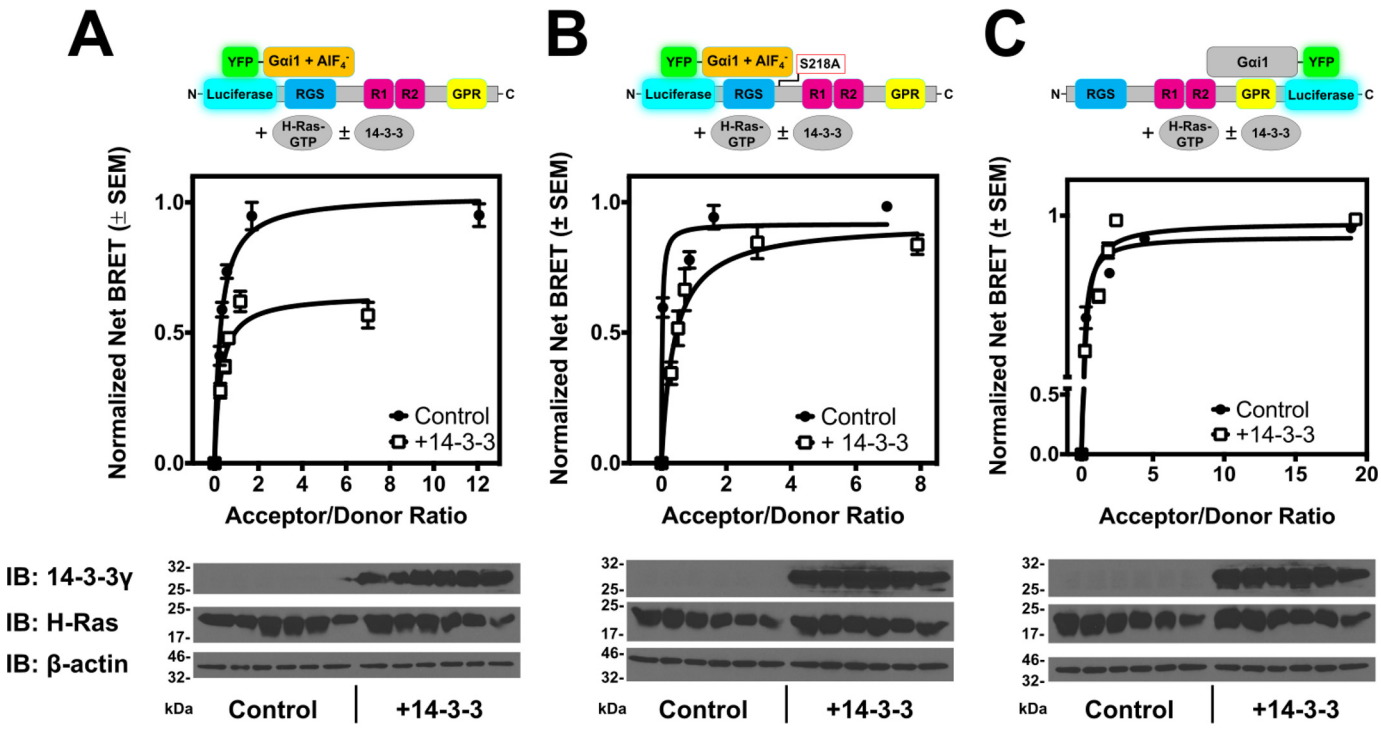

Figure 7. 14-3-3γ blocks $G\alpha_{i1}$ binding to the RGS14 RGS domain. *A* and *B*, HEK 293 cells were transfected with 5 ng of luciferase–RGS14 or 5 ng of luciferase–RGS14(S218A), increasing amounts of YFP–$G\alpha_{i1}$ (0, 25, 50, 100, 250, and 500 ng), and 250 ng of active H-Ras in the presence or absence of 500 ng of 14-3-3γ. $G\alpha_{i1}$ was activated with AlF_4^- for 30 min before BRET was measured. *C*, HEK 293 cells were transfected with 5 ng of RGS14–luciferase, increasing amounts of YFP–$G\alpha_{i1}$ (0, 25, 50, 100, 250, and 500 ng), and 250 ng of active H-Ras in the presence or absence of 500 ng of 14-3-3γ; $G\alpha_{i1}$ was not activated. For all experiments, BRET ratios were recorded, and the net BRET signal was calculated by subtracting the BRET signal from luciferase–RGS14 (*A* and *B*) or RGS14–luciferase (*C*) alone. Net BRET was normalized with maximum net BRET (0.0668 for *A*, 0.2768 for *B*, and 0.0607 for *C*) given a value of 1 and plotted against the acceptor (YFP)/donor (luciferase) ratio. Data shown are the pooled mean ± S.E. (*error bars*) of three separate experiments, each with triplicate determinations. Representative immunoblots showing expression levels of unlabeled proteins relevant to the experiments, H-Ras and 14-3-3γ, are shown below each BRET plot along with a β-actin loading control. Membranes were cut into strips to probe a single membrane with multiple antibodies. *IB*, immunoblotting.

ine 218) and RGS14 purified from *Escherichia coli*, which is assured to be unphosphorylated by mammalian kinases. Notably, 14-3-3γ directly binds RGS14 in both of these conditions (Fig. 10*A*), confirming the presence of a phosphorylation-independent 14-3-3–binding site on RGS14. To confirm that we were looking at a 14-3-3–binding site that is completely separate from the that centered at Ser-218 of RGS14, we created two truncation mutants of RGS14, RGS14(N-298) and RGS14(300-C), and partially purified them out of *E. coli*. We then performed far-Western blotting comparing direct binding of 14-3-3 to these truncations as well as full-length RGS14. 14-3-3γ interacts with full-length RGS14 and RGS14(300-C) but does not interact with RGS14(N-298) (Fig. 10*B*), confirming the presence of a second, phosphorylation-independent 14-3-3–binding site on RGS14 that is separate from the phosphorylation-dependent 14-3-3–binding site that requires Ser-218 phosphorylation.

Discussion

Here, we provide evidence that RGS14 directly interacts with 14-3-3 in both a phosphorylation-dependent and phosphorylation-independent manner. The phosphorylation-dependent interaction is markedly enhanced by downstream signaling through active H-Ras and is mediated by phosphorylation of serine 218 of RGS14, located adjacent to the RGS domain, in the linker region between the RGS domain and the R1 domain. Functionally, this interaction blocks active $G\alpha_i$ binding at the RGS domain but does not affect H-Ras binding to RGS14. Meanwhile, the phosphorylation-independent binding of 14-3-3 is correlated with the blockade of nuclear import of RGS14, thereby trapping it in the cytosol. One or both of these interactions take place within the mouse hippocampus, suggesting that 14-3-3 plays a role in regulating RGS14's suppression of synaptic plasticity in the CA2 region of the hippocampus.

H-Ras signaling promotes the specific phosphorylation-dependent interaction between RGS14 and 14-3-3

Our findings (Fig. 2) demonstrate that the 14-3-3 interaction with RGS14 is promoted by downstream signaling of active H-Ras independently of H-Ras binding directly to RGS14. As RGS14 interacts with Raf (45), a well known 14-3-3–binding partner (20, 23, 31, 46, 47), it was unclear to us whether 14-3-3 interacts directly with RGS14 or through an indirect interaction bridged by Raf. However, analysis by far-Western blotting showed that 14-3-3 is able to interact directly with RGS14 in the absence of any other RGS14-interacting partners (Fig. 3*B*). Furthermore, decreased interaction between RGS14 and 14-3-3 following treatment with λ-phosphatase indicated that 14-3-3 binds at a motif centered at a phosphorylated serine or threonine on RGS14 (Fig. 3). Mapping of the 14-3-3–binding site with truncation mutants of RGS14 followed by creation of phospho-null point mutants at potential 14-3-3–binding sites revealed a 14-3-3–binding site centered around serine 218 on

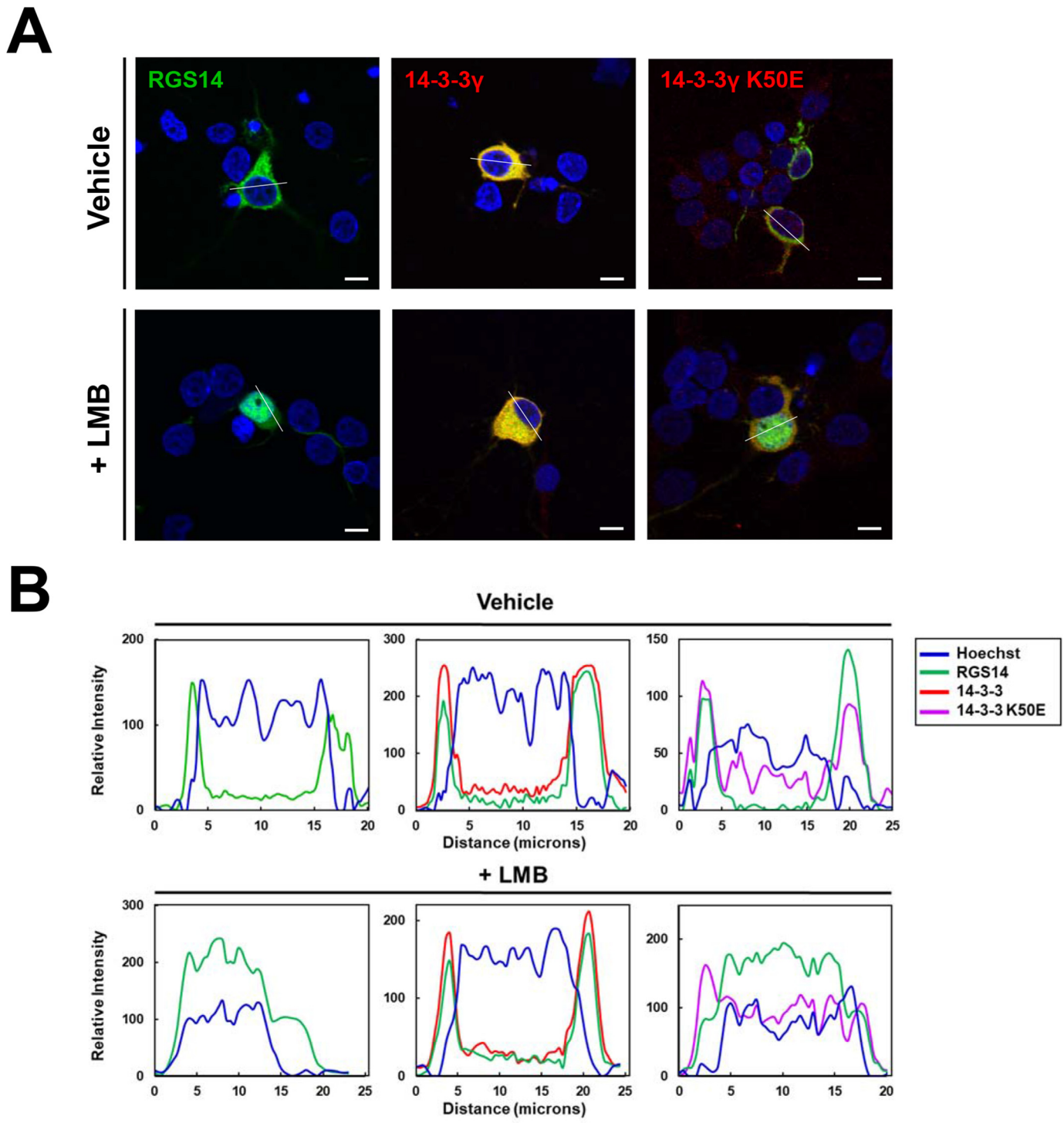

Figure 8. 14-3-3γ blocks RGS14 import into the nucleus of hippocampal neurons. *A*, primary neurons were transfected with 1 μg of YFP–RGS14 and 1 μg of empty vector, 1 μg of His-tagged 14-3-3γ, or 1 μg of His-tagged 14-3-3γ(K50E) per coverslip. Twenty-four hours later, neurons were treated with 40 nM leptomycin B (+*LMB*) or vehicle for 2 h before being fixed in 4% paraformaldehyde in PBS. YFP–RGS14 was visualized by the intrinsic fluorescence of YFP (*green*). 14-3-3γ immunostaining was performed using an anti-14-3-3γ primary antibody and Alexa Fluor 546 (*red*) secondary antibody, and nuclei were visualized by staining DNA with Hoechst 33258 (*blue*). Images are representative of at least three separate experiments. *Scale bars* represent 10 μm. *B*, relative fluorescence intensity of YFP–RGS14, 14-3-3, and nuclear staining was measured through a cross-section of each cell as indicated by the *white line* through each cell in *A*.

RGS14 in the linker region between the RGS and R1 domains (Figs. 4 and 5). This serine and the surrounding sequence are fully conserved among human, rat, and mouse RGS14, making it a likely candidate for 14-3-3 interaction and subsequent regulation of RGS14 activity (Fig. 5).

We next attempted to determine the kinase downstream of H-Ras that facilitates the interaction of 14-3-3 and RGS14 through the phosphorylation of serine 218 of RGS14. Although Scansite3 set on minimum stringency predicted the phosphorylation of serine 218 by CaMKII and Akt (50), which are both

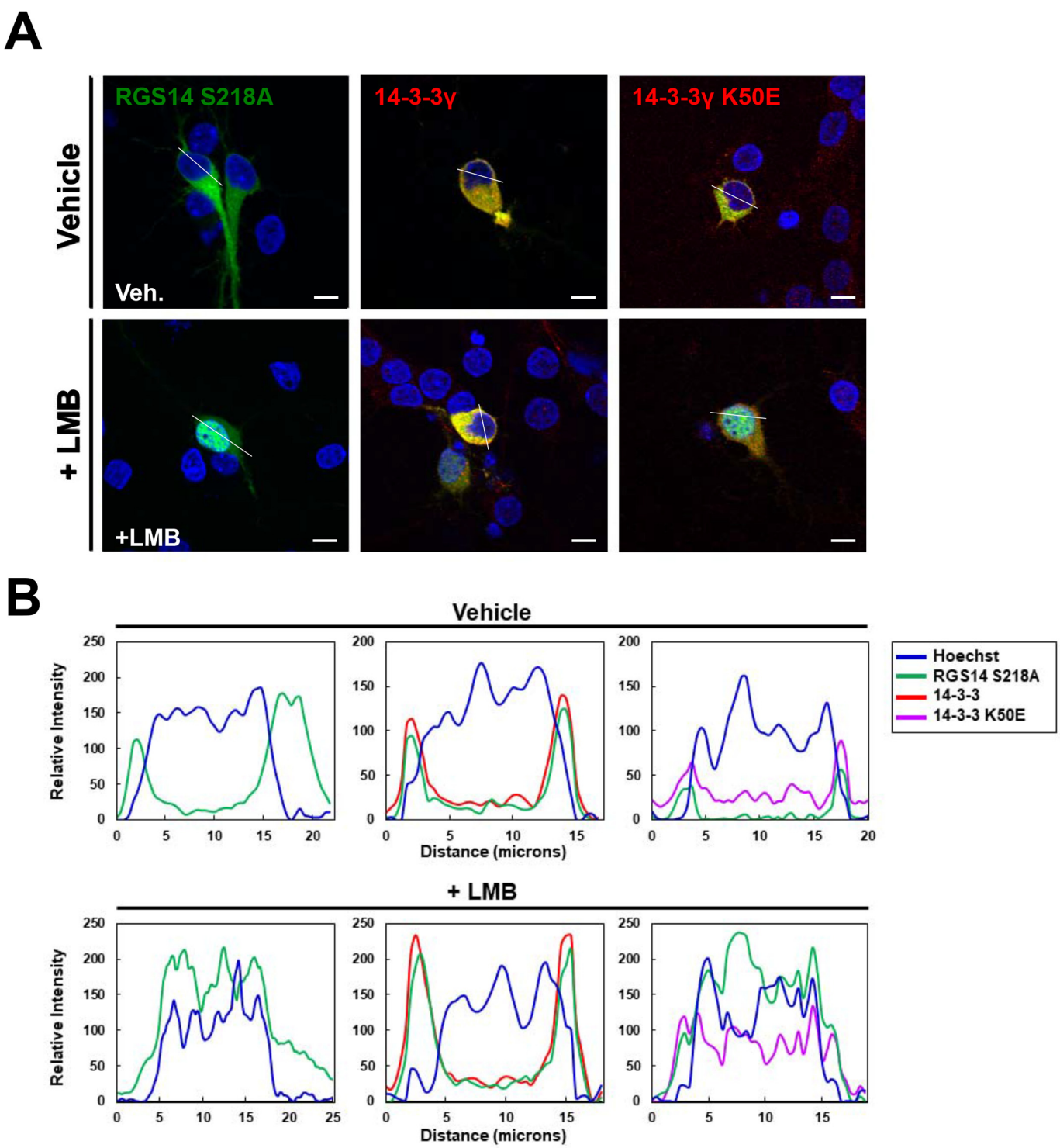

Figure 9. 14-3-3γ does not bind at serine 218 of RGS14 to block RGS14 import into the nucleus of hippocampal neurons. *A*, primary neurons were transfected with 1 μg of YFP–RGS14 and 1 μg of empty vector, 1 μg of His-tagged 14-3-3γ, or 1 μg of His-tagged 14-3-3γ(K50E) per coverslip. 24 h later, neurons were treated with 40 nM leptomycin B (+*LMB*) or vehicle (*Veh.*) for 2 h before being fixed in 4% paraformaldehyde in PBS. YFP–RGS14(S218A) was visualized by the intrinsic fluorescence of YFP (*green*). 14-3-3γ immunostaining was performed using an anti-14-3-3γ primary antibody and Alexa Fluor 546 (*red*) secondary antibody, and nuclei were visualized by staining DNA with Hoechst 33258 (*blue*). Images are representative of at least three separate experiments. *Scale bars* represent 10 μm. *B*, relative fluorescence intensity of YFP–RGS14(S218A), 14-3-3, and nuclear staining was measured through a cross-section of each cell as indicated by the *white line* through each cell in *A*.

activated downstream of H-Ras, treatment of cells with selective MEK, PI3K, and CaMKII inhibitors to block ERK, Akt, and CaMKII kinase activity, respectively, had no effect (Fig. S2*A*). Additional experiments showed that treatment of cells with EGF to activate kinases downstream of activated Ras, including ERK, does not begin to potentiate the interaction between RGS14 and 14-3-3 until approximately 2 h after treatment even though ERK activation occurs very rapidly (Fig. S2*B*). Taken

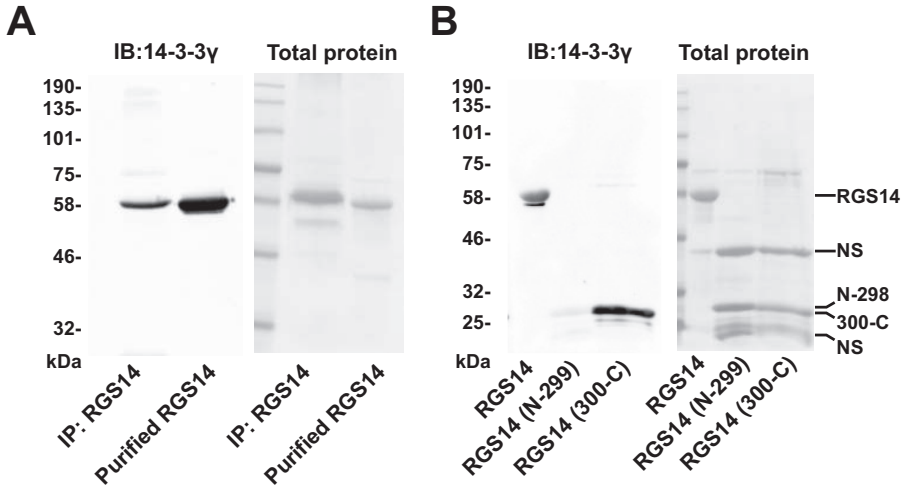

Figure 10. 14-3-3γ interacts with RGS14 at a unique binding site in a phosphorylation-independent manner. *A*, 9 μg of FLAG–RGS14 was expressed in HEK 293 cells and recovered by immunoprecipitation (*IP: RGS14*). 30% of the *IP: RGS14* sample and 5 μg of purified recombinant RGS14 expressed in *E. coli* (*Purified RGS14*) were subjected to SDS-PAGE and then transferred to a nitrocellulose membrane. The membrane (*left panel*) was incubated with pure His-tagged 14-3-3γ overnight and probed for interactions between RGS14 and 14-3-3 via immunoblotting for 14-3-3 (*IB: 14-3-3γ*). Equal amounts of the same protein samples were loaded in parallel on a separate gel and stained with Ponceau S (*right panel*) to show the relative abundance of the proteins in the immunoblot. *B*, 5 μg of RGS14, RGS14(N-298), and RGS14(300-C) partially purified from *E. coli* were subjected to SDS-PAGE and then transferred to a nitrocellulose membrane. The membrane (*left panel*) was incubated with pure His-tagged 14-3-3γ overnight and probed for interactions between RGS14 and 14-3-3 via immunoblotting for 14-3-3 (*IB: 14-3-3γ*). Equal amounts of the same protein samples were loaded in parallel on a separate gel and stained with Ponceau S (*right panel*) to show the relative abundance of the proteins in the immunoblot. *Lines* to the *right* of the *right panel* indicate the bands of RGS14 or truncations at the expected sizes in the Ponceau-stained membrane as well as nonspecific, unidentified proteins (*NS*) in the partially purified preparations. These findings are representative of three independent experiments.

together, these data suggest that active H-Ras enhancement of the interaction between RGS14 and 14-3-3 likely takes place due to long-term H-Ras activation, likely independent of ERK signaling, that influences changes in transcription and translation in the cell. These data coupled with the failure of the most highly predicted kinases to phosphorylate the 14-3-3–binding site on RGS14 makes identification of a kinase that phosphorylates serine 218 of RGS14 extremely difficult. Although the Scansite3 database takes many kinases into account, not all kinases are included, potentially excluding the kinase relevant to this discussion. Furthermore, there are many kinases for which there is no clear phosphorylation motif, making prediction of phosphorylation by those kinases difficult. H-Ras has many reported effectors that engage many more downstream kinases (56). Thus, at this time, we are unable to identify the kinase responsible for phosphorylating RGS14 at serine 218.

14-3-3 interaction with RGS14 inhibits active $G\alpha_i$ binding at the RGS domain

The interaction of 14-3-3 with target substrate proteins can elicit various effects, including conformational change, change in subcellular localization, and/or enhancement or inhibition of protein/protein interactions (16, 17, 19). Looking specifically at RGS proteins, 14-3-3 has been shown in several cases to inhibit Gα binding at the RGS domain (26, 35). These previously reported effects of 14-3-3 on RGS functions, coupled with the proximity of the RGS14 14-3-3–binding site adjacent to the RGS domain, led us to examine effects of 14-3-3 binding on RGS14 interactions with its known binding partners, active $G\alpha_{i/o}$, active H-Ras, and inactive $G\alpha_{i1}$. For these studies, ideally, we would examine the effects of 14-3-3 on direct protein/protein interactions using pure proteins to gain insight into the function of the RGS14/14-3-3 interaction. However, our inability to phosphorylate RGS14 *in vitro* with the appropriate kinase to promote 14-3-3 interaction limited this approach. In an attempt to mimic phosphorylation of RGS14 at serine 218, we replaced the residue with a phosphomimetic aspartate as well as glutamate. However, these phosphomimetic residues have been shown to be a poor mimic for a phosphate with respect to 14-3-3 binding (25, 57, 58), and these residue changes failed to promote 14-3-3 binding to RGS14 (data not shown). Therefore, with such limited options, we were forced to analyze interactions between RGS14 and associated proteins in live cells using BRET.

We first determined the effect of 14-3-3 interaction on the binding of active $G\alpha_i$ at the RGS domain and found that 14-3-3 does indeed decrease active $G\alpha_i$ interaction with the RGS domain, presumably inhibiting RGS14's negative regulation of $G\alpha_i$ downstream signaling. Because H-Ras signaling enhances 14-3-3 binding to RGS14 and 14-3-3 binds within the linker region between the RGS and Ras-binding domains of RGS14, we also examined the effect of 14-3-3 on H-Ras interaction with RGS14. Here, we saw no effect, indicating that 14-3-3 interactions with RGS14 selectively inhibit only active $G\alpha_i$ binding at the RGS domain, leaving intact RGS14 interaction with H-Ras at the R1 domain and inactive $G\alpha_i$ at the GPR motif. This selective inhibition by 14-3-3 of active $G\alpha_{i/o}$ interaction could function as a regulatory mechanism in which RGS14 could promote or enhance signaling through interactions at the R1 domain and GPR motif while selectively silencing RGS14 activity through the RGS domain.

RGS14 nuclear localization is prevented by phosphorylation-independent interaction with 14-3-3

A common function of 14-3-3 proteins is to affect the subcellular localization of their substrates (17, 21, 32, 34). Because

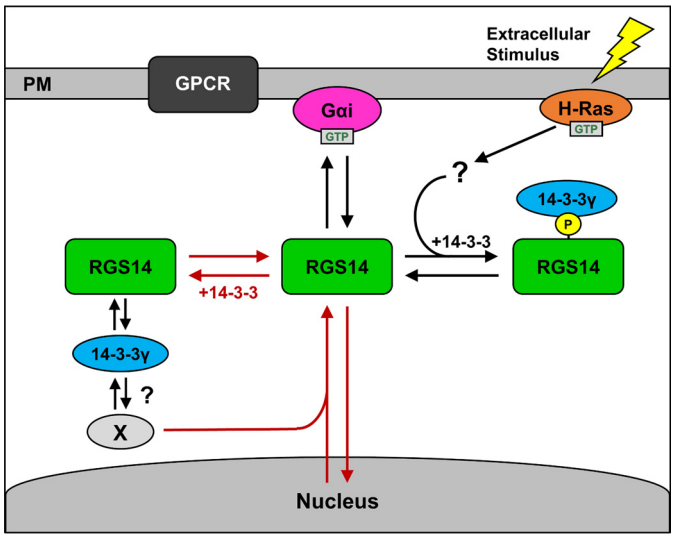

Figure 11. Proposed model showing bifunctional regulation of RGS14 by 14-3-3 contingent upon two different modes of binding. In resting cells, RGS14 exists in the cytoplasm, capable of shuttling in and out of the nucleus as well as interacting with active $G\alpha_i$–GTP at the plasma membrane (*PM*) via its RGS domain. Long-term H-Ras activation following an extracellular stimulus leads to the up-regulation and/or activation of an unidentified kinase, leading to phosphorylation of serine 218 of RGS14 and binding of 14-3-3γ at the motif centered around that residue. This phosphorylation-dependent binding disrupts RGS14 interaction with active $G\alpha_i$ at the plasma membrane while leaving interaction with other binding partners and nuclear localization unaffected (*black arrows*). RGS14 also interacts directly with 14-3-3γ in a phosphorylation-independent manner, possibly interacting directly with RGS14 to prevent RGS14 nuclear localization while not affecting interaction with active $G\alpha_i$–GTP (*red arrows*), although it is possible that 14-3-3 interacts with another binding partner to indirectly inhibit RGS14 nuclear localization.

we have previously shown that RGS14 shuttles in and out of the nucleus (5, 12, 14), we wanted to examine the effect of 14-3-3 interaction on RGS14 nuclear localization. Surprisingly, we found that 14-3-3 prevents RGS14 from translocating to the nucleus but that 14-3-3 binding at the phosphorylation-dependent binding site at serine 218 is not responsible for this effect (Figs. 8 and 9). Further examination showed that 14-3-3 is able to interact with RGS14 in a phosphorylation-independent manner at a unique 14-3-3– binding site on RGS14 (Fig. 10*B*), providing a bifunctional mechanism by which 14-3-3 can modulate RGS14 nuclear localization at one binding site while regulating active $G\alpha_i$ binding at another (Fig. 11). However, we should note that the phosphorylation-independent binding of 14-3-3 is only correlated with blockade of RGS14 nuclear import, and we cannot rule out the possibility that 14-3-3 may be interacting with other proteins to indirectly inhibit RGS14 transport into the nucleus.

Because this RGS14/14-3-3 interaction is not mediated by phosphorylation of a typical 14-3-3– binding site, there remains the question of how this interaction is regulated in the cell. RGS14 levels in the CA2 region of the hippocampus increase into adulthood and remain stable (41). However, 14-3-3 expression has been shown to change based on conditions in the cell (59). It is possible that expression levels of 14-3-3 may be a unique mechanism by which RGS14 nuclear localization is regulated. Insight into the actual function of 14-3-3's blockade of RGS14 nuclear localization is limited at this time because a function for RGS14 in the nucleus has not yet been determined.

Endogenous RGS14 interacts with 14-3-3 in mouse hippocampus

Within the brain, RGS14 is selectively expressed in the CA2 subregion of the hippocampus (41) where it has been shown to suppress synaptic plasticity and associated learning and memory (3). Importantly, we found that endogenous RGS14 and 14-3-3 can form a stable complex in this part of the brain as shown via coimmunoprecipitation of 14-3-3 with RGS14 from isolated mouse hippocampus (Fig. 1). 14-3-3γ, the 14-3-3 isoform that selectively interacts with RGS14 (Fig. S1), is highly expressed in hippocampal neurons as well (60), putting this isoform in position to regulate RGS14 function. Of note, 14-3-3 proteins are also linked to synaptic plasticity. Functional knockout of 14-3-3 has been shown to inhibit hippocampal LTP and associative learning and memory (18). Additionally, 14-3-3 proteins have been shown to be necessary for activation of the Ras/Raf/MEK/ERK signaling pathway (20, 47), which we show here *indirectly* promotes the phosphorylation-dependent interaction between RGS14 and 14-3-3. Furthermore, this signaling cascade has been shown to be necessary for normal synaptic plasticity and the expression of LTP (61) behind mammalian associative learning (62), which native RGS14 has been shown to suppress in the CA2 region (3). Additionally, it is unclear where and how RGS14 is acting to suppress LTP. Phosphorylation-independent interaction between RGS14 and 14-3-3 could regulate the balance of RGS14 in the cytoplasm and nucleus, changing RGS14's distribution to either reduce or enhance its suppression of LTP in the hippocampus. Because of the effect of 14-3-3 on RGS14's subcellular localization (Figs. 8 and 9) and interaction with functional binding partners, we speculate that 14-3-3 interactions could regulate RGS14 suppression of synaptic plasticity.

Conclusions and future directions

Here, we show that RGS14 interacts with a novel binding partner, 14-3-3, in both a phosphorylation-dependent and phosphorylation-independent manner. The phosphorylation-dependent interaction is promoted by signaling downstream of activated H-Ras. This interaction specifically inhibits interaction of active $G\alpha_{i/o}$ at the RGS domain while leaving association with active H-Ras and inactive $G\alpha_i$ unperturbed. Meanwhile, 14-3-3 also binds within the C-terminal half of RGS14 in a phosphorylation-independent manner and blocks (either directly or indirectly) RGS14 import into the nucleus of neurons. These interactions provide novel mechanisms of regulation of RGS14 interactions and localization, respectively, that give us further insight into RGS14 function in its native environment, the hippocampus, where we demonstrated that endogenous RGS14 interacts with native 14-3-3. Furthermore, both H-Ras and 14-3-3 have been shown to play critical roles in the proper expression of LTP with RGS14 suppressing this form of synaptic plasticity. Future studies will be directed at determining whether and how H-Ras signaling in CA2 pyramidal neurons functions to control phosphorylation-dependent RGS14/14-3-3 interactions. Also of great interest is understanding the role of RGS14 in the nucleus and 14-3-3's role in blocking RGS14 localization there. To our knowledge, this is the first report

demonstrating 14-3-3–mediated inhibition of RGS protein nuclear translocation, although the possibility has been suggested for other RGS proteins (36, 63). Multiple other RGS proteins have been found in the nucleus, including RGS3 (64), RGS6 (65), RGS7 (66, 67), RGS9-2 (67), RGS10 (68, 69), and RGS12 (70, 71). It is possible that 14-3-3 acts similarly on all of these RGS proteins, preventing their nuclear import. Future studies elucidating the conditions necessary for phosphorylation-dependent and -independent RGS14:14-3-3 complex formation will allow us to understand whether and how 14-3-3 plays a definitive role in RGS14 regulation of synaptic plasticity.

Experimental procedures

Plasmids and antibodies

Rat RGS14 cDNA (GenBank™ accession number U92279) used throughout this study was obtained as described previously (4). The plasmids encoding full-length FLAG–RGS14 in pcDNA3.1 (Invitrogen) as well as FLAG–RGS14 truncation mutants encompassing residues 1–202, 205–490, 371–544, and 444–544 were created as described previously (5). The plasmid encoding rat RGS14 cDNA was used to generate Luc–RGS14 and RGS14–Luc constructs in the phRLucN2 vector as described previously (6). The plasmid encoding His_6–MBP–TEV–RGS14 in a pLIC-MBP vector was obtained as described previously (9). His_6–MBP–TEV–RGS14(300-C) was cloned into the pLIC-MBP vector using ligation-independent cloning with the following primers: forward, 5′-TAC TTC CAA TCC AAT GCG ATG AAG TAC TGC TGC GTG TAT CTA CC-3′; reverse, 5′-TTA TCC ACT TCC AAT GCG CTA TGG AAG GAC CAG GTC CTC TTT GCG-3′. His_6–MBP–TEV–RGS14(N-298) was created by inserting a stop codon at residue 299 of full-length RGS14 in the same vector using the QuikChange kit (Stratagene) with the following primers: forward, 5′-AGC GAA AGC CGG CCC TAG AAG TAC TGC TGC GTG-3′; reverse, 5′-CAC GCA GCA GTA CTT CTA GGG CCG GCT TTC GCT-3′. RGS14(R333L), which demonstrates decreased binding to active H-Ras at the R1 domain, was created as described previously (45). The FLAG–RGS14 (S258A) construct used to probe for a potential 14-3-3– binding site was generated with the QuikChange kit using the following primers: forward, 5′-GCC CTG CGA CGA GAG GCT CAG GGA TCC CTG AAT TCT TCC GCG-3′; reverse, 5′-CGC GGA AGA ATT CAG GGA TCC CTG AGC CTC TCG TCG CAG GGC. The FLAG–RGS14(S286A) construct used to probe for a potential 14-3-3– binding site was generated using the QuikChange kit and the following primers: forward, 5′-GTG AGC AGC AAA TCC GAG AGC CAC CGA AAG GCC CTT GGA AGT GGA GAG GGT GAG-3′; reverse, 5′-CTC ACC CTC TCC ACT TCC AAG GGC CTT TCG GTG GCT CTC GGA TTT GCT GCT CAC-3′. The FLAG–RGS14(S218A) construct in which serine 218 was replaced with phospho-null alanine to prevent binding of 14-3-3 at that residue was generated with the QuikChange kit using the following primers: forward, 5′-CCA AAG CTG AAG CCT GGA AAG GCA CTG CCG CTC GGT GTG GAA GAG-3′; reverse, 5′-CTC TTC CAC ACC GAG CGG CAG TGC CTT TCC AGG CTT CAG CTT TGG-3′. The Luc–RGS14(S218A) and YFP–RGS14(S218A) constructs were created using the same primers and QuikChange kit. The FLAG–RGS14 truncation from residues 1–380 was created by mutating the codon for leucine 381 to a stop codon using the QuikChange kit and the following primers: forward, 5′-GCT GGA GTT GGT CGG CTA GGA GCG TGT GGT ACG GAT CTC TGC TAA GCC C-3′; reverse, 5′-GGG CTT AGC AGA GAT CCG TAC CAC ACG CTC CTA GCC GAC CAA CTC CAG C-3′. The FLAG–RGS14 truncation from residues 1–300 was created by mutating the codon for tyrosine 301 to a stop codon using the QuikChange kit and the following primers: forward, 5′-CGG CCC GGG AAG TAA TGC TGC GTG TAT C-3′; reverse, 5′-GAT ACA CGC AGC ATT ACT TCC CGG GCC G-3′. Rat YFP–$G\alpha_{i1}$ in pcDNA3.1 was generated by Dr. Scott Gibson (72). 3xHA-tagged (N terminus) WT H-Ras plasmid and inactive (S17N) mutant as well as untagged active H-Ras(G12V) were purchased from the cDNA Resource Center (Bloomsburg, PA). 14-3-3γ, -β, -τ, and -ζ cDNA constructs in pcDNA3.1 were graciously provided by Dr. Haian Fu (Emory University) along with the binding-incompetent 14-3-3γ(K50E) construct. Antisera used include anti-penta-His (Qiagen, 34660), anti-14-3-3 (Santa Cruz Biotechnology Inc., sc-629), anti-14-3-3γ (Santa Cruz Biotechnology, Inc., sc-398423), anti-H-Ras (Santa Cruz Biotechnology, Inc., sc-520), anti-phospho-p44/42 mitogen-activated protein kinase (Cell Signaling Technology, Inc., 9101), HRP-conjugated anti-FLAG (Sigma, A8592), HRP-conjugated goat anti-mouse IgG (Rockland Immunochemicals, 610-1302), HRP-conjugated goat anti-rabbit IgG (Bio-Rad, 1706515), and Alexa Fluor 546 goat anti-mouse IgG (Thermo Fisher, A11030).

Immunoblotting

Protein samples in Laemmli buffer were loaded onto 11% acrylamide gels, and proteins were resolved via SDS-PAGE before being transferred onto a nitrocellulose membrane. Membranes were blocked at room temperature for 1 h at 4 °C overnight in buffer containing 5% nonfat milk (w/v), 0.1% Tween 20, and 0.02% sodium azide in 20 mM TBS, pH 7.6. Membranes were then incubated with primary antibody in the same buffer, except for anti-FLAG, for 2 h at room temperature or overnight at 4 °C. Membranes were washed three times for 8 min with TBS containing 0.1% Tween 20 (TBST) before being incubated with either anti-mouse or anti-rabbit HRP-conjugated secondary antibody diluted in TBST (1:5,000 and 1:25,000, respectively) for 45 min at room temperature. Membranes being blotted for FLAG were incubated with anti-FLAG HRP-conjugated primary antibody for 45 min immediately after blocking. Following incubation with HRP-conjugated primary or secondary antibody, membranes were washed three times for 8 min each in TBST before visualizing protein bands using enhanced chemiluminescence and exposing membranes to X-ray films.

Ponceau red stain stock was made from 20 mg/ml Ponceau S in water. Membranes were stained in a 1:100 stock-to-water dilution for 5 min before being rinsed in water and imaged.

Cell culture and transfection

HEK 293 cells were incubated in 1× Dulbecco's modified Eagle's medium with phenol red pH indicator supplemented with 10% fetal bovine serum and 100 units/ml each penicillin and streptomycin. Cells were maintained at 37 °C in 5% CO_2. Transfections were carried out using polyethyleneimine (PEI) as described previously (73).

Our protocol for culturing neurons was adapted from Beaudoin *et al.* (74). Brains were removed from E18–19 embryos obtained from a timed pregnant Sprague-Dawley rat (Charles River). All animal housings and procedures were approved by the Emory University Institutional Animal Care and Use Committee (IACUC), and all procedures were approved by IACUC protocol. The meninges were removed, and the hippocampi were isolated in calcium- and magnesium-free HBSS (Invitrogen) supplemented with 1× sodium pyruvate (Invitrogen), 0.1% glucose (Sigma-Aldrich), and 10 mM HEPES (Sigma-Aldrich), pH 7.3. Isolated hippocampi were washed with the HBSS solution and then dissociated using the same buffer containing 0.25% trypsin (Worthington) for 8 minutes at 37 °C. Trypsinized hippocampi were washed two times with the same HBSS buffer before being triturated five to six times with a fire-polished glass Pasteur pipette in basal medium Eagle (Invitrogen) supplemented with 10% fetal bovine serum (VWR), 0.45% glucose (Sigma-Aldrich), 1× sodium pyruvate (Invitrogen), 1× GlutaMAX (Invitrogen), and 1× penicillin/streptomycin (HyClone). Neurons were counted and plated at a density of 80,000 cells/cm^2 in basal medium Eagle–based buffer on coverslips that had been etched with 70% nitric acid (Sigma-Aldrich) before being coated with 1 mg/ml poly-L-lysine (Sigma-Aldrich) in borate buffer. Cells were allowed to adhere for 1–3 h before medium was changed to Neurobasal (Invitrogen) supplemented with 1× B27 (Invitrogen) and 1× GlutaMAX (Invitrogen). Neurons were kept in a 37 °C, 5% CO_2 incubator, and half of the medium was replaced with new Neurobasal every 3–4 days until neurons were used for experiments.

Neurons were transfected using a calcium phosphate transfection kit (Clontech) with a protocol adapted from Jiang and Chen (75). Briefly, calcium solution containing DNA was slowly added to an equal volume of HEPES-buffered saline to form calcium phosphate precipitate containing the DNA. This precipitate was added to neurons on coverslips that had been placed in new wells in new medium. Neurons were incubated with precipitate for 1.5 h before dissolving the precipitate with slightly acidified medium that had been equilibrated in a 10% CO_2 incubator for 15–20 min. Cells were placed back in the 5% CO_2 incubator. After this incubation, coverslips were placed back in their original well in their original culture medium.

RGS14 immunoprecipitation from mouse hippocampus

Brains from C57BL6 WT mice were removed, and hippocampi were isolated by dissection. Hippocampi were homogenized using a Dounce homogenizer in lysis buffer containing 50 mM Tris, pH 7.05, 150 mM NaCl, 1 mM EDTA, 2 mM DTT, 5 mM $MgCl_2$, 1 EDTA-free cOmplete mini protease inhibitor tablet (Roche Applied Science) at 1× concentration, 1× Halt phosphatase inhibitor mixture (Thermo Scientific), and 1% Triton X-100. Brain lysate was incubated on a rotator at 4 °C for 1 h and then cleared by spinning it down at 13,000 rpm for 10 min. Protein G-Sepharose beads (GE Healthcare) were preblocked with 3% bovine serum albumin (BSA) before lysate was added. Half of the brain lysate was incubated with 50 μl of preblocked beads in the absence of RGS14 antibody, and the other half of the lysate was incubated with 50 μl of beads along with 5 μl (1.63 μg) of anti-RGS14 (Proteintech) antibody for 2 h on a rotator at 4 °C. Immunocomplexes were then washed four times with PBS containing 0.1% Tween 20 before being boiled off the beads in 2× Laemmli buffer for 5 min. Samples were then resolved via SDS-PAGE and subjected to immunoblotting for analysis. All animal housings and procedures were approved by the Emory University IACUC, and all procedures were approved by IACUC protocol.

FLAG immunoprecipitation

Twenty-four hours following transfection, cells were washed twice in ice-cold PBS and collected in lysis buffer of the same composition used for RGS14 immunoprecipitation from mouse brain. Lysates were rotated at 4 °C for 1 h. Lysates were cleared by spinning down samples at 13,000 rpm for 10 min with 30 μl put aside to determine total cell lysate expression of proteins of interest, and the remaining supernatant was incubated with anti-FLAG M2 affinity gel (Sigma), which was previously blocked in 3% BSA in PBS for 1 h. Cleared lysates were rotated at 4 °C for 1.5 h. Immunocomplexes were then washed three times with 1 ml of PBS containing 0.1% Tween 20 before being suspended in 2× Laemmli buffer, boiled for 5 min, resolved by 11% SDS-PAGE, and transferred to a nitrocellulose membrane for immunoblotting.

Purification of recombinant proteins

RGS14 and truncated RGS14 (N-298 and 300-C) were expressed in *E. coli* and partially purified as described previously (9). Recombinant hexahistidine–14-3-3γ was expressed from a pDEST17-based plasmid in BL21(DE3) *E. coli* cells and purified using Ni^{2+}-affinity chromatography in the manner described previously (76) with minor modifications. Specifically, cells were lysed using sonication instead of a French pressure cell. Purified protein was snap frozen in liquid nitrogen and stored in aliquots at −80 °C until use.

λ-Phosphatase treatment of lysates

FLAG immunoprecipitation was performed as described above with the exception of the addition of 1× Halt phosphatase inhibitor mixture. Before washing the immunocomplexes and eluting samples, the anti-FLAG affinity gel was resuspended in fresh lysis buffer with the addition of 2 mM $MnCl_2$ and 900 units of Mn^{2+}-dependent λ-phosphatase and rotated at room temperature for 1 h to cleave phosphate groups from potentially phosphorylated serine and threonine residues. Following treatment with phosphatase, lysates were washed, eluted, and analyzed as described above.

Blot overlay "far-Western blotting"

HEK 293 cells were transfected with FLAG–RGS14 in the presence or absence of active H-Ras using PEI. Twenty-four

hours after transfection, FLAG–RGS14 and associated proteins were isolated via FLAG immunoprecipitation, resolved by SDS-PAGE, and transferred to a nitrocellulose membrane. The membrane was then treated with pure His-tagged 14-3-3γ at 7.5 μg/ml in a buffer containing 50 mM Tris, 50 mM NaCl, and 2 mM DTT on a rocking incubator at 4 °C overnight. The membrane was then immunoblotted as described above for 14-3-3 to determine whether 14-3-3 directly bound the RGS14 in the membrane.

BRET

BRET experiments were performed as described previously (6, 9). Briefly, HEK 293 cells were transfected with a donor and acceptor as well as any additional constructs using PEI. To determine whether 14-3-3 affects active H-Ras association with RGS14, we expressed H-Ras(G12V)–Venus with RGS14–Luc or RGS14(S218A)–Luc in the presence or absence of 14-3-3γ. To measure YFP–$G\alpha_{i1}$ interactions with the RGS14 RGS domain, Luc–RGS14 was expressed, whereas YFP–$G\alpha_{i1}$ interactions with the RGS14 GPR motif were measured using RGS14–Luc because the RGS domain and GPR motif are closer to the N and C termini of RGS14, respectively. Luc–RGS14(S218A) was used as a negative control to determine the effect of 14-3-3 interaction with RGS14 on active YFP–$G\alpha_{i1}$ binding at the RGS domain. Twenty-four hours after transfection, cells were suspended in Tyrode's solution containing 140 mM NaCl, 5 mM KCl, 1 mM $MgCl_2$, 1 mM $CaCl_2$, 0.37 mM NaH_2PO_4, 24 mM $NaHCO_3$, 10 mM HEPES, and 0.1% glucose, pH 7.4. Cells treated with AlF_4^- were harvested in Tyrode's solution containing the addition of 10 mM NaF, 9 mM $MgCl_2$, and 30 μM $AlCl_3$ for 30 min before readings were taken. Cells were plated onto white 96-well OptiPlates (PerkinElmer Life Sciences). Acceptor expression was determined by measuring fluorescence using a TriStar LB 941 plate reader (Berthold Technologies) with 485- and 530-nm excitation and emission filters, respectively. BRET was measured using 485- and 530-nm emission filters after a 2-min application of 5 μM coelenterazine H (Nanolight Technologies). The change in BRET (net BRET) was determined by dividing the 530 nm (YFP) signal by the 485 nm (Luc) signal and subtracting the signal from Luc–RGS14 or RGS14–Luc alone. All data were collected using MikroWin 2000 software and analyzed in Microsoft Excel followed by GraphPad Prism.

Kinase inhibitor treatments

HEK 293 cells were treated with the MEK inhibitor U0126 (Sigma) at 10 μM, the PI3K inhibitor LY294002 (Sigma) at 50 μM, or the CaMKII inhibitor KN-93 (Sigma) at 100 μM for 2 h before cells were collected and lysed. Samples were then submitted to FLAG immunoprecipitation before being analyzed via immunoblotting.

EGF treatment of cells

HEK 293 cells were treated with EGF (Sigma) at 100 ng/ml for 0, 10, 60, or 120 min before being collected and lysed for FLAG immunoprecipitation.

Leptomycin B treatment of cells and immunocytochemistry

Primary hippocampal neurons were treated with LMB (Sigma) at 40 ng/ml or vehicle (70% ethanol) for 2 h before being fixed for 15 min in 4% paraformaldehyde in 1× PBS. Cells were then permeabilized for 10 min in PBS containing 0.1% Triton X-100 and incubated in 8% BSA in PBS blocking buffer for 1 h before being incubated with primary antibody in 4% BSA in PBS for 2 h. Following three washes with 0.05% Triton X-100 in PBS, coverslips were incubated with secondary antibody in 4% BSA in PBS for 1 h before being stained with 1.6 μM Hoechst dye (Thermo Fisher) for 4 min. Coverslips were then washed three times in PBS before being mounted on slides using ProLong Diamond antifade mountant (Thermo Fisher). Images were taken on an Olympus FV1000 inverted confocal microscope at 100× and then processed using ImageJ software. Approximately 10 images per condition were obtained, and representative images are shown.

Author contributions—K. J. G. and J. R. H. conceptualization; K. J. G. and K. E. S. data curation; K. J. G. and K. E. S. formal analysis; K. J. G. and J. R. H. funding acquisition; K. J. G. validation; K. J. G. and K. E. S. investigation; K. J. G. visualization; K. J. G. and K. E. S. methodology; K. J. G. writing-original draft; K. J. G., K. E. S., and J. R. H. writing-review and editing; J. R. H. resources; J. R. H. supervision; J. R. H. project administration.

Acknowledgments—We thank Dr. Haian Fu (Emory University, Atlanta, GA) for the very generous contribution of the 14-3-3 plasmids used for this study. We also thank Suneela Ramineni for outstanding technical assistance. The Emory University Integrated Cellular Imaging Microscopy Core of the Emory Neuroscience was supported by NINDS, National Institutes of Health Core Facilities Grant 5P30NS055077.

References

1. Ross, E. M., and Wilkie, T. M. (2000) GTPase-activating proteins for heterotrimeric G proteins: regulators of G protein signaling (RGS) and RGS-like proteins. *Annu. Rev. Biochem.* **69,** 795–827 CrossRef Medline
2. Hollinger, S., and Hepler, J. R. (2002) Cellular regulation of RGS proteins: modulators and integrators of G protein signaling. *Pharmacol. Rev.* **54,** 527–559 CrossRef Medline
3. Lee, S. E., Simons, S. B., Heldt, S. A., Zhao, M., Schroeder, J. P., Vellano, C. P., Cowan, D. P., Ramineni, S., Yates, C. K., Feng, Y., Smith, Y., Sweatt, J. D., Weinshenker, D., Ressler, K. J., Dudek, S. M., *et al.* (2010) RGS14 is a natural suppressor of both synaptic plasticity in CA2 neurons and hippocampal-based learning and memory. *Proc. Natl. Acad. Sci. U.S.A.* **107,** 16994–16998 CrossRef Medline
4. Hollinger, S., Taylor, J. B., Goldman, E. H., and Hepler, J. R. (2001) RGS14 is a bifunctional regulator of Gαi/o activity that exists in multiple populations in brain. *J. Neurochem.* **79,** 941–949 Medline
5. Shu, F. J., Ramineni, S., Amyot, W., and Hepler, J. R. (2007) Selective interactions between Giα1 and Giα3 and the GoLoco/GPR domain of RGS14 influence its dynamic subcellular localization. *Cell. Signal.* **19,** 163–176 CrossRef Medline
6. Vellano, C. P., Brown, N. E., Blumer, J. B., and Hepler, J. R. (2013) Assembly and function of the regulator of G protein signaling 14 (RGS14)·H-Ras signaling complex in live cells are regulated by $G\alpha_{i1}$ and $G_{\alpha i}$-linked G protein-coupled receptors. *J. Biol. Chem.* **288,** 3620–3631 CrossRef Medline
7. Willard, F. S., Willard, M. D., Kimple, A. J., Soundararajan, M., Oestreich, E. A., Li, X., Sowa, N. A., Kimple, R. J., Doyle, D. A., Der, C. J., Zylka, M. J., Snider, W. D., and Siderovski, D. P. (2009) Regulator of G-protein signal-

ing 14 (RGS14) is a selective H-Ras effector. *PLoS One* **4,** e4884 CrossRef Medline
8. Traver, S., Bidot, C., Spassky, N., Baltauss, T., De Tand, M. F., Thomas, J. L., Zalc, B., Janoueix-Lerosey, I., and Gunzburg, J. D. (2000) RGS14 is a novel Rap effector that preferentially regulates the GTPase activity of Gαo. *Biochem. J.* **350,** 19–29 Medline
9. Brown, N. E., Goswami, D., Branch, M. R., Ramineni, S., Ortlund, E. A., Griffin, P. R., and Hepler, J. R. (2015) Integration of G protein α (Gα) signaling by the regulator of G protein signaling 14 (RGS14). *J. Biol. Chem.* **290,** 9037–9049 CrossRef Medline
10. Brown, N. E., Lambert, N. A., and Hepler, J. R. (2016) RGS14 regulates the lifetime of Gα-GTP signaling but does not prolong Gβγ signaling following receptor activation in live cells. *Pharmacol. Res. Perspect.* **4,** e00249 CrossRef Medline
11. Vellano, C. P., Maher, E. M., Hepler, J. R., and Blumer, J. B. (2011) G protein-coupled receptors and resistance to inhibitors of cholinesterase-8A (Ric-8A) both regulate the regulator of G protein signaling 14 RGS14·$G\alpha_{i1}$ complex in live cells. *J. Biol. Chem.* **286,** 38659–38669 CrossRef Medline
12. Branch, M. R., and Hepler, J. R. (2017) Endogenous RGS14 is a cytoplasmic-nuclear shuttling protein that localizes to juxtanuclear membranes and chromatin-rich regions of the nucleus. *PLoS One* **12,** e0184497 CrossRef Medline
13. Squires, K. E., Gerber, K. J., Pare, J. F., Branch, M. R., Smith, Y., and Hepler, J. R. (2018) Regulator of G protein signaling 14 (RGS14) is expressed pre- and postsynaptically in neurons of hippocampus, basal ganglia, and amygdala of monkey and human brain. *Brain Struct. Funct.* **223,** 233–253 CrossRef Medline
14. Cho, H., Kim, D. U., and Kehrl, J. H. (2005) RGS14 is a centrosomal and nuclear cytoplasmic shuttling protein that traffics to promyelocytic leukemia nuclear bodies following heat shock. *J. Biol. Chem.* **280,** 805–814 Medline
15. Aitken, A. (1995) 14-3-3 proteins on the MAP. *Trends Biochem. Sci.* **20,** 95–97 CrossRef Medline
16. Fu, H., Subramanian, R. R., and Masters, S. C. (2000) 14-3-3 proteins: structure, function, and regulation. *Annu. Rev. Pharmacol. Toxicol.* **40,** 617–647 CrossRef Medline
17. Yaffe, M. B. (2002) How do 14-3-3 proteins work?—Gatekeeper phosphorylation and the molecular anvil hypothesis. *FEBS Lett.* **513,** 53–57 CrossRef Medline
18. Qiao, H., Foote, M., Graham, K., Wu, Y., and Zhou, Y. (2014) 14-3-3 proteins are required for hippocampal long-term potentiation and associative learning and memory. *J. Neurosci.* **34,** 4801–4808 CrossRef Medline
19. Tzivion, G., Shen, Y. H., and Zhu, J. (2001) 14-3-3 proteins; bringing new definitions to scaffolding. *Oncogene* **20,** 6331–6338 CrossRef Medline
20. Tzivion, G., Luo, Z., and Avruch, J. (1998) A dimeric 14-3-3 protein is an essential cofactor for Raf kinase activity. *Nature* **394,** 88–92 CrossRef Medline
21. Yuan, H., Michelsen, K., and Schwappach, B. (2003) 14-3-3 dimers probe the assembly status of multimeric membrane proteins. *Curr. Biol.* **13,** 638–646 CrossRef Medline
22. Yaffe, M. B., Rittinger, K., Volinia, S., Caron, P. R., Aitken, A., Leffers, H., Gamblin, S. J., Smerdon, S. J., and Cantley, L. C. (1997) The structural basis for 14-3-3:phosphopeptide binding specificity. *Cell* **91,** 961–971 CrossRef Medline
23. Petosa, C., Masters, S. C., Bankston, L. A., Pohl, J., Wang, B., Fu, H., and Liddington, R. C. (1998) 14-3-3ζ binds a phosphorylated Raf peptide and an unphosphorylated peptide via its conserved amphipathic groove. *J. Biol. Chem.* **273,** 16305–16310 CrossRef Medline
24. Molzan, M., and Ottmann, C. (2012) Synergistic binding of the phosphorylated S233- and S259-binding sites of C-RAF to one 14-3-3ζ dimer. *J. Mol. Biol.* **423,** 486–495 CrossRef Medline
25. Muslin, A. J., Tanner, J. W., Allen, P. M., and Shaw, A. S. (1996) Interaction of 14-3-3 with signaling proteins is mediated by the recognition of phosphoserine. *Cell* **84,** 889–897 CrossRef Medline
26. Abramow-Newerly, M., Ming, H., and Chidiac, P. (2006) Modulation of subfamily B/R4 RGS protein function by 14-3-3 proteins. *Cell. Signal.* **18,** 2209–2222 CrossRef Medline
27. Campbell, J. K., Gurung, R., Romero, S., Speed, C. J., Andrews, R. K., Berndt, M. C., and Mitchell, C. A. (1997) Activation of the 43 kDa inositol polyphosphate 5-phosphatase by 14-3-3ζ. *Biochemistry* **36,** 15363–15370 CrossRef Medline
28. Fu, H., Coburn, J., and Collier, R. J. (1993) The eukaryotic host factor that activates exoenzyme S of *Pseudomonas aeruginosa* is a member of the 14-3-3 protein family. *Proc. Natl. Acad. Sci. U.S.A.* **90,** 2320–2324 CrossRef Medline
29. Masters, S. C., Pederson, K. J., Zhang, L., Barbieri, J. T., and Fu, H. (1999) Interaction of 14-3-3 with a nonphosphorylated protein ligand, exoenzyme S of *Pseudomonas aeruginosa*. *Biochemistry* **38,** 5216–5221 CrossRef Medline
30. Alam, R., Hachiya, N., Sakaguchi, M., Kawabata, S., Iwanaga, S., Kitajima, M., Mihara, K., and Omura, T. (1994) cDNA cloning and characterization of mitochondrial import stimulation factor (MSF) purified from rat liver cytosol. *J. Biochem.* **116,** 416–425 CrossRef Medline
31. Clark, G. J., Drugan, J. K., Rossman, K. L., Carpenter, J. W., Rogers-Graham, K., Fu, H., Der, C. J., and Campbell, S. L. (1997) 14-3-3ζ negatively regulates Raf-1 activity by interactions with the Raf-1 cysteine-rich domain. *J. Biol. Chem.* **272,** 20990–20993 CrossRef Medline
32. Nufer, O., and Hauri, H. P. (2003) ER export: call 14-3-3. *Curr. Biol.* **13,** R391–R393 CrossRef Medline
33. Obsil, T., Ghirlando, R., Klein, D. C., Ganguly, S., and Dyda, F. (2001) Crystal structure of the 14-3-3ζ:serotonin N-acetyltransferase complex. a role for scaffolding in enzyme regulation. *Cell* **105,** 257–267 CrossRef Medline
34. O'Kelly, I., Butler, M. H., Zilberberg, N., and Goldstein, S. A. (2002) Forward transport. 14-3-3 binding overcomes retention in endoplasmic reticulum by dibasic signals. *Cell* **111,** 577–588 CrossRef Medline
35. Benzing, T., Yaffe, M. B., Arnould, T., Sellin, L., Schermer, B., Schilling, B., Schreiber, R., Kunzelmann, K., Leparc, G. G., Kim, E., and Walz, G. (2000) 14-3-3 interacts with regulator of G protein signaling proteins and modulates their activity. *J. Biol. Chem.* **275,** 28167–28172 CrossRef Medline
36. Niu, J., Scheschonka, A., Druey, K. M., Davis, A., Reed, E., Kolenko, V., Bodnar, R., Voyno-Yasenetskaya, T., Du, X., Kehrl, J., and Dulin, N. O. (2002) RGS3 interacts with 14-3-3 via the N-terminal region distinct from the RGS (regulator of G-protein signalling) domain. *Biochem. J.* **365,** 677–684 CrossRef Medline
37. Rezabkova, L., Boura, E., Herman, P., Vecer, J., Bourova, L., Sulc, M., Svoboda, P., Obsilova, V., and Obsil, T. (2010) 14-3-3 protein interacts with and affects the structure of RGS domain of regulator of G protein signaling 3 (RGS3). *J. Struct. Biol.* **170,** 451–461 CrossRef Medline
38. Rezabkova, L., Man, P., Novak, P., Herman, P., Vecer, J., Obsilova, V., and Obsil, T. (2011) Structural basis for the 14-3-3 protein-dependent inhibition of the regulator of G protein signaling 3 (RGS3) function. *J. Biol. Chem.* **286,** 43527–43536 CrossRef Medline
39. Benzing, T., Köttgen, M., Johnson, M., Schermer, B., Zentgraf, H., Walz, G., and Kim, E. (2002) Interaction of 14-3-3 protein with regulator of G protein signaling 7 is dynamically regulated by tumor necrosis factor-α. *J. Biol. Chem.* **277,** 32954–32962 CrossRef Medline
40. Hollinger, S., Ramineni, S., and Hepler, J. R. (2003) Phosphorylation of RGS14 by protein kinase A potentiates its activity toward Gαi. *Biochemistry* **42,** 811–819 CrossRef Medline
41. Evans, P. R., Lee, S. E., Smith, Y., and Hepler, J. R. (2014) Postnatal developmental expression of regulator of G protein signaling 14 (RGS14) in the mouse brain. *J. Comp. Neurol.* **522,** 186–203 CrossRef Medline
42. Zhang, L., Wang, H., Liu, D., Liddington, R., and Fu, H. (1997) Raf-1 kinase and exoenzyme S interact with 14-3-3ζ through a common site involving lysine 49. *J. Biol. Chem.* **272,** 13717–13724 CrossRef Medline
43. Jin, Y., Dai, M. S., Lu, S. Z., Xu, Y., Luo, Z., Zhao, Y., and Lu, H. (2006) 14-3-3γ binds to MDMX that is phosphorylated by UV-activated Chk1, resulting in p53 activation. *EMBO J.* **25,** 1207–1218 CrossRef Medline
44. Snow, B. E., Antonio, L., Suggs, S., Gutstein, H. B., and Siderovski, D. P. (1997) Molecular cloning and expression analysis of rat Rgs12 and Rgs14. *Biochem. Biophys. Res. Commun.* **233,** 770–777 CrossRef Medline

45. Shu, F. J., Ramineni, S., and Hepler, J. R. (2010) RGS14 is a multifunctional scaffold that integrates G protein and Ras/Raf MAPkinase signalling pathways. *Cell. Signal.* **22,** 366–376 CrossRef Medline
46. Li, S., Janosch, P., Tanji, M., Rosenfeld, G. C., Waymire, J. C., Mischak, H., Kolch, W., and Sedivy, J. M. (1995) Regulation of Raf-1 kinase activity by the 14-3-3 family of proteins. *EMBO J.* **14,** 685–696 Medline
47. Roy, S., McPherson, R. A., Apolloni, A., Yan, J., Lane, A., Clyde-Smith, J., and Hancock, J. F. (1998) 14-3-3 facilitates Ras-dependent Raf-1 activation *in vitro* and *in vivo*. *Mol. Cell. Biol.* **18,** 3947–3955 CrossRef Medline
48. Light, Y., Paterson, H., and Marais, R. (2002) 14-3-3 antagonizes Ras-mediated Raf-1 recruitment to the plasma membrane to maintain signaling fidelity. *Mol. Cell. Biol.* **22,** 4984–4996 CrossRef Medline
49. Fischer, A., Baljuls, A., Reinders, J., Nekhoroshkova, E., Sibilski, C., Metz, R., Albert, S., Rajalingam, K., Hekman, M., and Rapp, U. R. (2009) Regulation of RAF activity by 14-3-3 proteins: RAF kinases associate functionally with both homo- and heterodimeric forms of 14-3-3 proteins. *J. Biol. Chem.* **284,** 3183–3194 CrossRef Medline
50. Obenauer, J. C., Cantley, L. C., and Yaffe, M. B. (2003) Scansite 2.0: proteome-wide prediction of cell signaling interactions using short sequence motifs. *Nucleic Acids Res.* **31,** 3635–3641 CrossRef Medline
51. Hornbeck, P. V., Zhang, B., Murray, B., Kornhauser, J. M., Latham, V., and Skrzypek, E. (2015) PhosphoSitePlus, 2014: mutations, PTMs and recalibrations. *Nucleic Acids Res.* **43,** D512–D520 CrossRef Medline
52. Demirkan, G., Yu, K., Boylan, J. M., Salomon, A. R., and Gruppuso, P. A. (2011) Phosphoproteomic profiling of *in vivo* signaling in liver by the mammalian target of rapamycin complex 1 (mTORC1). *PLoS One* **6,** e21729 CrossRef Medline
53. Lundby, A., Secher, A., Lage, K., Nordsborg, N. B., Dmytriyev, A., Lundby, C., and Olsen, J. V. (2012) Quantitative maps of protein phosphorylation sites across 14 different rat organs and tissues. *Nat. Commun.* **3,** 876 CrossRef Medline
54. Pinto, S. M., Nirujogi, R. S., Rojas, P. L., Patil, A. H., Manda, S. S., Subbannayya, Y., Roa, J. C., Chatterjee, A., Prasad, T. S., and Pandey, A. (2015) Quantitative phosphoproteomic analysis of IL-33-mediated signaling. *Proteomics* **15,** 532–544 CrossRef Medline
55. Mayya, V., Lundgren, D. H., Hwang, S. I., Rezaul, K., Wu, L., Eng, J. K., Rodionov, V., and Han, D. K. (2009) Quantitative phosphoproteomic analysis of T cell receptor signaling reveals system-wide modulation of protein-protein interactions. *Sci. Signal.* **2,** ra46 CrossRef Medline
56. Rajalingam, K., Schreck, R., Rapp, U. R., and Albert, S. (2007) Ras oncogenes and their downstream targets. *Biochim. Biophys. Acta* **1773,** 1177–1195 CrossRef Medline
57. Johnson, C., Crowther, S., Stafford, M. J., Campbell, D. G., Toth, R., and MacKintosh, C. (2010) Bioinformatic and experimental survey of 14-3-3-binding sites. *Biochem. J.* **427,** 69–78 CrossRef Medline
58. Astuti, P., and Gabrielli, B. (2011) Phosphorylation of Cdc25B3 Ser169 regulates 14-3-3 binding to Ser151 and Cdc25B activity. *Cell Cycle* **10,** 1960–1967 CrossRef Medline
59. Chen, J., Lee, C. T., Errico, S. L., Becker, K. G., and Freed, W. J. (2007) Increases in expression of 14-3-3 eta and 14-3-3ζ transcripts during neuroprotection induced by Δ9-tetrahydrocannabinol in AF5 cells. *J. Neurosci. Res.* **85,** 1724–1733 CrossRef Medline
60. Baxter, H. C., Liu, W. G., Forster, J. L., Aitken, A., and Fraser, J. R. (2002) Immunolocalisation of 14-3-3 isoforms in normal and scrapie-infected murine brain. *Neuroscience* **109,** 5–14 CrossRef Medline
61. English, J. D., and Sweatt, J. D. (1997) A requirement for the mitogen-activated protein kinase cascade in hippocampal long term potentiation. *J. Biol. Chem.* **272,** 19103–19106 CrossRef Medline
62. Atkins, C. M., Selcher, J. C., Petraitis, J. J., Trzaskos, J. M., and Sweatt, J. D. (1998) The MAPK cascade is required for mammalian associative learning. *Nat. Neurosci.* **1,** 602–609 CrossRef Medline
63. Burchett, S. A. (2003) In through the out door: nuclear localization of the regulators of G protein signaling. *J. Neurochem.* **87,** 551–559 CrossRef Medline
64. Dulin, N. O., Pratt, P., Tiruppathi, C., Niu, J., Voyno-Yasenetskaya, T., and Dunn, M. J. (2000) Regulator of G protein signaling RGS3T is localized to the nucleus and induces apoptosis. *J. Biol. Chem.* **275,** 21317–21323 CrossRef Medline
65. Chatterjee, T. K., and Fisher, R. A. (2003) Mild heat and proteotoxic stress promote unique subcellular trafficking and nucleolar accumulation of RGS6 and other RGS proteins. Role of the RGS domain in stress-induced trafficking of RGS proteins. *J. Biol. Chem.* **278,** 30272–30282 CrossRef Medline
66. Rose, J. J., Taylor, J. B., Shi, J., Cockett, M. I., Jones, P. G., and Hepler, J. R. (2000) RGS7 is palmitoylated and exists as biochemically distinct forms. *J. Neurochem.* **75,** 2103–2112 CrossRef Medline
67. Witherow, D. S., Wang, Q., Levay, K., Cabrera, J. L., Chen, J., Willars, G. B., and Slepak, V. Z. (2000) Complexes of the G protein subunit Gβ5 with the regulators of G protein signaling RGS7 and RGS9. Characterization in native tissues and in transfected cells. *J. Biol. Chem.* **275,** 24872–24880 CrossRef Medline
68. Lee, J. K., and Tansey, M. G. (2015) Physiology of RGS10 in neurons and immune cells. *Prog. Mol. Biol. Transl. Sci.* **133,** 153–167 CrossRef Medline
69. Burgon, P. G., Lee, W. L., Nixon, A. B., Peralta, E. G., and Casey, P. J. (2001) Phosphorylation and nuclear translocation of a regulator of G protein signaling (RGS10). *J. Biol. Chem.* **276,** 32828–32834 CrossRef Medline
70. Chatterjee, T. K., and Fisher, R. A. (2000) Novel alternative splicing and nuclear localization of human RGS12 gene products. *J. Biol. Chem.* **275,** 29660–29671 CrossRef Medline
71. Chatterjee, T. K., and Fisher, R. A. (2002) RGS12TS-S localizes at nuclear matrix-associated subnuclear structures and represses transcription: structural requirements for subnuclear targeting and transcriptional repression. *Mol. Cell. Biol.* **22,** 4334–4345 CrossRef Medline
72. Gibson, S. K., and Gilman, A. G. (2006) Giα and Gβ subunits both define selectivity of G protein activation by α2-adrenergic receptors. *Proc. Natl. Acad. Sci. U.S.A.* **103,** 212–217 CrossRef Medline
73. Oner, S. S., Maher, E. M., Breton, B., Bouvier, M., and Blumer, J. B. (2010) Receptor-regulated interaction of activator of G-protein signaling-4 and $G\alpha_i$. *J. Biol. Chem.* **285,** 20588–20594 CrossRef Medline
74. Beaudoin, G. M., 3rd, Lee, S. H., Singh, D., Yuan, Y., Ng, Y. G., Reichardt, L. F., and Arikkath, J. (2012) Culturing pyramidal neurons from the early postnatal mouse hippocampus and cortex. *Nat. Protoc.* **7,** 1741–1754 CrossRef Medline
75. Jiang, M., and Chen, G. (2006) High Ca^{2+}-phosphate transfection efficiency in low-density neuronal cultures. *Nat. Protoc.* **1,** 695–700 CrossRef Medline
76. Bernstein, L. S., Ramineni, S., Hague, C., Cladman, W., Chidiac, P., Levey, A. I., and Hepler, J. R. (2004) RGS2 binds directly and selectively to the M1 muscarinic acetylcholine receptor third intracellular loop to modulate $G_{q/11}\alpha$ signaling. *J. Biol. Chem.* **279,** 21248–21256 CrossRef Medline